CLEARED
FOR PUBLIC RELEASE
PL/PA 16 DEC 96

Sensor and Simulation Notes

Note 136

August 1971

# A Cylindrical Post Above a Perfectly Conducting Plate, II (Dynamic Case)

by

Lennart Marin
Northrop Corporate Laboratories
Pasadena, California

## Abstract

The time behavior and frequency variation are obtained of the total current induced on a cylindrical post above a ground plane by a step-function plane wave traveling above the ground plane. The late time behavior of the current is quite accurately determined by the resonant frequency and decay time constant of the fundamental mode of the post together with its associated peak current. The resonant frequency, the decay time constant and the field enhancement factor, the latter quantity being defined as the ratio of the maximum induced total charge to the late time induced total charge on the end caps of the post, are calculated for various values of the post-to-ground plate separation. The frequency variation and time history of the total charge induced on the end caps of the post are also graphed for several values of the post-to-ground plane separation.

PL 96-0951

## I. Introduction

This study is a continuation of previous studies[1,2,3,4,5,6] on the electromagnetic interaction of a parallel-plate simulator and a post inside it. In a previous note[4] we have studied in great detail the electrostatic interaction of one post above a ground plane. Here, we will continue our investigation into the response of the post to a step-function incident plane wave traveling above the ground plane. Particular attention will be paid to the effect of the plate-to-post separation for one given value of the post's diatmeter-to-length ratio on the total current induced on the post. It is shown that the late-time behavior of the current can be determined quite accurately in terms of the resonant frequency and decay time constant of the fundamental mode of the post together with its associated peak current amplitude. Another quantity of interest is the total charge induced on each end cap of the post. Of particular importance is the field enhancement factor, defined as the ratio of the maximum induced total charge to the late-time induced total charge on the end caps of the post, when the post is exposed to a step-function incident wave.

In section II we derive an integral equation for the total current on the post by applying Green's theorem to axial symmetric bodies. This integral equation is then solved numerically in section III by making use of numerical quadrature formulas. The numerical results are presented in section IV in graphical form for the variation of the post current (I) with frequency at five different positions on the post and (2) along the post at resonant frequency. For several post-to-plate separations we graph the time behavior of the total current induced on the post at five different positions for a step-function incident plane wave. In section IV we also tabulate the field enhancement factor and graph the frequency variation and time history of the total charge induced on the post's ends for several values of the post-to-plate separation.

## II. Integral Equation for the Post Current

Following the procedure in reference 1 we have the following integral equation for the $\phi$-symmetric part of the tangential component of the magnetic field, $H_\phi(\rho,z)$, on the post

$$f(\rho,z)H_\phi(\rho,z) + \int_o^a K_1(\rho,z,\rho',d)H_\phi(\rho',d)\rho'd\rho' - \int_d^b K_2(\rho,z,a,z')H_\phi(a,z')dz'$$

$$- \int_o^a K_1(\rho,z,\rho',b)H_\phi(\rho',b)\rho'd\rho' = H_\phi^{inc}(\rho,z) \qquad (1)$$

where

$$f(\rho,z) = \begin{cases} 1/2, & \text{if } (|\rho - a| + |z - d|)(|\rho - a| + |z - b|) \neq 0 \\ 3/4, & \text{if } (|\rho - a| + |z - d|)(|\rho - a| + |z - b|) = 0, \end{cases}$$

$$K_1(\rho,z,\rho',z') = \frac{\partial}{\partial z'}[G(\rho,z,\rho',z')],$$

$$K_2(\rho,z,\rho',z') = -\frac{\partial}{\partial \rho'}[\rho'G(\rho,z,\rho',z')]$$

and $H_\phi^{inc}(\rho,z)$ is the incident field averaged with respect to $\phi$. The Green's function, $G(\rho,z,\rho',z')$, satisfies the differential equation

$$\left[\frac{\partial^2}{\partial\rho^2} + \frac{1}{\rho}\frac{\partial}{\partial\rho} - \frac{1}{\rho^2} + \frac{\partial^2}{\partial z^2} + k^2\right]G = -\frac{\delta(\rho-\rho')}{\rho'}\delta(z - z') \qquad (2)$$

for $z > 0$ and the boundary condition

$$\frac{\partial G}{\partial z} = 0 \qquad \text{when } z = 0.$$

From the theory of images it follows that G has the following form

$$G(\rho,z,\rho',z') = \frac{1}{4\pi}\int_o^{2\pi}\left[\frac{e^{ikR_+}}{R_+} + \frac{e^{ikR_-}}{R_-}\right]\cos\psi d\psi \qquad (3)$$

where

$$R_{\pm} = [\rho^2 + \rho'^2 - 2\rho\rho' \cos\psi + (z \pm z')^2]^{\frac{1}{2}}.$$

For an incident harmonic plane wave given by

$$\underline{H}^{inc} = - \hat{y} H_o e^{ikx}$$

we have

$$H_\phi^{inc}(\rho,z) = - iH_o J_1(k\rho), \tag{4}$$

$J_1(x)$ being the Bessel function of the first kind and order one. In terms of the current, $I(\rho,z)$, defined by

$$I(\rho,z) = 2\pi\rho H_\phi(\rho,z), \tag{5}$$

equation (1) becomes

$$f(\rho,z)I(\rho,z) + \int_o^a \rho K_1(\rho,z,\rho',d)I(\rho',d)d\rho' - \int_d^b \rho K_2(\rho,z,a,z')I(a,z')dz'$$

$$- \int_o^a \rho K_1(\rho,z,\rho',b)I(\rho',b)d\rho' = - 2\pi i\rho J_1(k\rho). \tag{6}$$

In the next section we will discuss the numerical solution of (6).

## III. Numerical Solution of the Integral Equation for the Current

The integrals on the left hand side of (6) can be approximated by the following sums

$$\int_o^a \rho K_1(\rho,z,\rho',d)I(\rho',d)d\rho' \approx \sum_{j=1}^{N_1} \rho K_1(\rho,z,\rho_j,z_j)I(\rho_j,z_j)w_j, \tag{7}$$

$$\rho_j = a[1 + \xi_j(N_1)]/2,\ z_j = d,\ w_j = ar_j(N_1)/2$$

$$\int_d^b \rho K_2(\rho,z,a,z')I(a,z')dz' \approx \sum_{j=M_1}^{M_2} L(\rho,z,\rho_j,z_j)I(\rho_j,z_j), \tag{8}$$

$$\rho_j = a,\ z_j = 2(j - M_1)\Delta$$

$$\int_o^a \rho K_1(\rho,z,\rho',b)I(\rho',b)d\rho' \approx \sum_{j=M_3}^{N} \rho K_1(\rho,z,\rho_j,z_j)I(\rho_j,z_j)w_j, \tag{9}$$

$$\rho_j = a[1 + \xi_{j-M_3}(N_3)]/2,\ z_j = b,\ w_j = ar_{j-M_3}(N_3)/2$$

In equations (7) and (9) we have made use of the Gaussian integration formula. The abscissas, $\xi_j(n)$, and weight factors, $r_j(n)$, in the Gaussian integration formula using n sample points on the interval (-1,1) are given by[6]

$$P_n[\xi_j(n)] = 0$$

$$r_j(n) = 2/\left\{[1 - \xi_j^2][P_n'(\xi_j)]^2\right\}$$

where $P_n(\xi)$ is the Legendre polynomial of degree n. Dividing the cylindrical surface into $N_2$ zones (see figure 2) and assuming that the current is constant on each zone we arrive at (8) where

$$\Delta = (b - d)/[2(N_2 - 1)],$$

$$L(\rho,z,\rho_j,z_j) = \int_{-\delta_j}^{\Delta_j} \rho K_2(\rho,z,\rho_j,z_j + v)dv,$$

$$\Delta_j = \begin{cases} \Delta, & M_1 \le j \le M_2 - 1 \\ 0, & j = M_2 \end{cases}$$

$$\delta_j = \begin{cases} 0, & j = M_1 \\ \Delta, & M_1 + 1 \le j \le M_2. \end{cases}$$

Moreover,

$$M_1 = N_1 + 1$$

$$M_2 = N_1 + N_2$$

$$M_3 = M_2 + 1$$

$$N = N_1 + N_2 + N_3$$

Approximating the left hand side of (6) by the sums (7) through (9) and equating the sum thus obtained to the right hand side of (6) at N points $(\rho_\ell,z_\ell)$ we can form the following system of algebraic equations for the integral equation (6)

$$f_\ell I_\ell + \sum_{j=1}^{N} K_{\ell j} I_j = -2\pi i \rho_\ell J_1(k\rho_\ell), \qquad 1 \le \ell \le N \tag{10}$$

where

$$f_\ell = f(\rho_\ell,z_\ell)$$

For $\ell \neq j$ we have

$$K_{\ell j} = \begin{cases} [P(\rho_\ell,\rho_j,z_j + z_\ell) + P(\rho_\ell,\rho_j,z_j - z_\ell)]w_j, & 1 \le j \le N_1 \\ \int_{-\delta_j}^{\Delta_j} [Q(\rho_\ell,\rho_j,z_j + z_\ell + v) + Q(\rho_\ell,\rho_j,z_j - z_\ell + v)]dv, & M_1 \le j \le M_2 \\ -[P(\rho_\ell,\rho_j,z_j + z_\ell) + P(\rho_\ell,\rho_j,z_j - z_\ell)]w_j, & M_3 \le j \le N \end{cases}$$

and

$$K_{\ell\ell} = \begin{cases} P(\rho_\ell,\rho_\ell,2z_\ell)w_\ell, & 1 \le \ell \le N_1 \\ [F_1 + F_2 + F_3](\Delta_\ell - \delta_\ell)/\Delta + \int_{-\delta_\ell}^{\Delta_\ell} Q(\rho_\ell,\rho_\ell,2z_\ell + v)dv, & M_1 \le \ell \le M_2 \\ - P(\rho_\ell,\rho_\ell,2z_\ell)w_\ell, & M_3 \le \ell \le N \end{cases}$$

where

$$P(\rho,\rho',\zeta) = \pi^{-1}\rho \int_o^{\pi/2} \zeta(1 - ikR)R^{-3}e^{ikR} \cos 2\phi d\phi ,$$

$$Q(\rho,\rho',\zeta) = \pi^{-1}\rho \int_o^{\pi/2} (\rho - \rho' \cos 2\phi)(1 - ikR)R^{-3}e^{ikR}\, d\phi ,$$

$$R = (\rho^2 + \rho'^2 - 2\rho\rho' \cos 2\phi + \zeta^2)^{\frac{1}{2}} ,$$

$$F_1 = 2a^2\pi^{-1} \int_o^{\pi/2}\int_o^{\Delta} [(1 - ikR_a)e^{ikR_a} - 1 - k^2R_a^2/2]R_a^{-3} \sin^2\phi d\phi dv ,$$

$$F_2 = \Delta[2\pi(\Delta^2 + 4a^2)^{\frac{1}{2}}]^{-1} K[2a(\Delta^2 + 4a^2)^{-\frac{1}{2}}] ,$$

$$F_3 = .25\, k^2a^2\left\{-.5 + \ln(\Delta/a) + (4/\pi) \int_o^{\pi/2} \ln[1 + (1 + 4a^2\Delta^{-2} \sin^2\phi)^{\frac{1}{2}}]\sin^2\phi d\phi\right\} ,$$

$$R_a = (v^2 + 4a^2 \sin^2\phi)^{\frac{1}{2}}.$$

K(x) is the complete elliptic integral of the first kind

$$K(x) = \int_o^{\pi/2} (1 - x^2 \sin^2\phi)^{-\frac{1}{2}} \, d\phi \, .$$

The system of equations (10) was solved numerically on an electronic computer (CDC 6600) and the results of these calculations will be discussed in the next section.

## IV. Numerical Results

### A. The Induced Current on the Post

The system of equations (10), which approximates the integral equation (6) for the induced post current, was solved numerically for a/h = .1 and several values of d/h. Figures 3 through 7 are plots of the post current with d/h as a parameter at different points on the cylindrical surface. A normalized quantity, u, defined by

$$u = (z - d - h)/h$$

(see figure 2) has been used in the graphs of the normalized current, $I_1(u,k)$, so that $I_1(u,k) = |I(a,z)|/(hH_o)$. From these curves we see that the resonant frequency of the dominant mode decreases as the distance between the post and the ground plane decreases. The variation with d/h of the resonant frequency, $f_1$, of the dominant mode normalized with respect to its value, $f_{1\infty}$, for d/h = ∞ is given in table 1 and figure 8. In figure 9 the magnitude of the post current at resonant frequency is plotted versus the normalized position u.

For a step-function incident plane wave with the magnetic field vector

$$\underline{H}^{inc}(x,t) = -\hat{y}H_o U[t - (x + a)/c]$$

the time history of the normalized post current, $i_1(u,t)$, is plotted in figures 10 through 14 for u = -1, -.5, 0, .5, 1 and with d/h as parameter, where $i_1(u,t) = i(u,t)/(hH_o)$ and i(u,t) is the total post current. For late times the induced post current can be described by means of the resonant frequency, $f_1$, and the time decay constant, $\tau_1$, of the dominant mode. These two quantities, normalized with respect to their values for d/h = ∞ are graphed in figure 8 and tabulated in table 1.

### B. The Induced Surface Charge on the Ends of the Post

To estimate the field strength near the ends of the post we will calculate

the total charge induced on the end caps of the post. Integrating the continuity equation

$$\nabla \cdot \underline{K} + \frac{\partial \sigma}{\partial t} = 0,$$

where $\underline{K}$ is the surface current density and $\sigma$ is the surface charge density over each end cap of the post we immediately get

$$q(-1,t) = -\int_0^t i(-1,t')dt'$$

$$q(1,t) = \int_0^t i(1,t')dt'$$

where $q(\pm 1,t)$ is the total charge induced on the upper and lower end cap of the post, respectively. In the frequency domain we have

$$Q(\pm 1,k) = \pm(ick)^{-1} I(\pm 1,k),$$

where c is the velocity of light. Figures 15 and 16 are graphs of the frequency variation of the normalized induced surface charge,

$$Q_1(\pm 1,k) = |Q(\pm 1,k)|/(\varepsilon_o E_o h^2),$$

on the ends of the post and figures 17 and 18 display the time history of the same quantities,

$$q_1(\pm 1,t) = q(\pm 1,t)/(\varepsilon_o E_o h^2).$$

In table 2 we give the variation with d/h of

$$q_s(\pm 1) = \lim_{k\to 0} |Q(\pm 1,k)|/(\varepsilon_o E_o h^2),$$

$$q_r(\pm 1) = |Q(\pm 1,k_1)|/[\varepsilon_o E_o h^2 q_s(\pm 1)],$$

$$q_m(\pm 1) = |Q(\pm 1, t_m)|/[\varepsilon_o E_o h^2 q_s(\pm 1)],$$

$$c_s(\pm 1) = q_s(\pm 1)/q_{s\infty}(\pm 1),$$

$$c_r(\pm 1) = q_r(\pm 1)/q_{r\infty}(\pm 1),$$

$$c_m(\pm 1) = q_m(\pm 1)/q_{m\infty}(\pm 1)$$

where $k_1 = 2\pi f_1/c$, $t_m$ is the first zero crossing in the time-history curves of the current, $E_o$ is the magnitude of the electric field of the incident plane wave and a quantity with subscript $\infty$ denotes the value of this quantity for $d/h = \infty$. The normalized quantities $c_s(\pm 1)$, $c_r(\pm 1)$ and $c_m(\pm 1)$ are graphed in figures 19 and 20. Notice that $q_r$ and $q_m$ correspond to $C_r/C_s$ and $C_m/C_s$ in reference 2, respectively, and that one can call $q_r$ the field enhancement factor at the first resonant frequency and $q_m$ the maximum enhancement factor. Moreover, $c_s(\pm 1)$ corresponds to $C_s/C_o$ in reference 3.

Table 1. The resonant frequency and time decay constant of the dominant mode.

| $d/h$ | $k_o h$ | $k_o/k_{o\infty}$ | $c\tau_1/h$ | $\tau_1/\tau_{1\infty}$ |
|---|---|---|---|---|
| 0 | .65 | .50 | 11.2 | 2.38 |
| .02 | .95 | .73 | 5.6 | 1.19 |
| .05 | 1.05 | .81 | 4.5 | .96 |
| .10 | 1.10 | .85 | 4.0 | .85 |
| .25 | 1.25 | .96 | 3.5 | .74 |
| .50 | 1.30 | 1.00 | 3.2 | .68 |
| 1.00 | 1.30 | 1.00 | 4.5 | .98 |
| 2.00 | 1.30 | 1.00 | 4.9 | 1.04 |
| 5.00 | 1.30 | 1.00 | 4.8 | 1.02 |
| 10.00 | 1.30 | 1.00 | 4.7 | 1.00 |
| $\infty$ | 1.30 | 1.00 | 4.7 | 1.00 |

Table 2. The induced surface charge on the ends of the post.

| d/h | $q_s(1)$ | $c_s(1)$ | $q_s(-1)$ | $c_s(-1)$ | $q_r(1)$ | $c_r(1)$ | $q_r(-1)$ | $c_r(-1)$ | $q_m(1)$ | $c_m(1)$ | $q_m(-1)$ | $c_m(-1)$ | $t_m$ |
|---|---|---|---|---|---|---|---|---|---|---|---|---|---|
| 0 | .390 | 1.36 | -- | -- | 3.66 | 1.36 | -- | -- | 1.91 | 1.27 | -- | -- | 4.3 |
| .02 | .352 | 1.23 | 1.182 | 4.12 | 2.32 | .86 | 2.85 | 1.06 | 1.39 | .92 | 1.61 | 1.07 | 3.2 |
| .05 | .327 | 1.14 | .651 | 2.27 | 2.17 | .80 | 2.60 | .96 | 1.39 | .92 | 1.58 | 1.05 | 2.6 |
| .10 | .309 | 1.08 | .441 | 1.54 | 2.08 | .77 | 2.42 | .90 | 1.40 | .93 | 1.55 | 1.03 | 2.5 |
| .25 | .297 | 1.04 | .330 | 1.15 | 2.07 | .77 | 2.27 | .84 | 1.45 | .96 | 1.50 | .99 | 2.3 |
| .50 | .292 | 1.02 | .301 | 1.05 | 2.20 | .82 | 2.27 | .84 | 1.48 | .98 | 1.48 | .98 | 2.3 |
| 1.00 | .289 | 1.01 | .291 | 1.01 | 2.61 | .97 | 2.53 | .94 | 1.49 | .99 | 1.49 | .98 | 2.3 |
| 2.00 | .288 | 1.00 | .288 | 1.00 | 2.79 | 1.03 | 2.77 | 1.03 | 1.50 | .99 | 1.50 | .99 | 2.3 |
| 5.00 | .287 | 1.00 | .287 | 1.00 | 2.70 | 1.00 | 2.71 | 1.01 | 1.51 | 1.00 | 1.51 | 1.00 | 2.3 |
| 10.00 | .287 | 1.00 | .287 | 1.00 | 2.70 | 1.00 | 2.70 | 1.00 | 1.51 | 1.00 | 1.51 | 1.00 | 2.3 |
| $\infty$ | .287 | 1.00 | .287 | 1.00 | 2.70 | 1.00 | 2.70 | 1.00 | 1.51 | 1.00 | 1.51 | 1.00 | 2.3 |

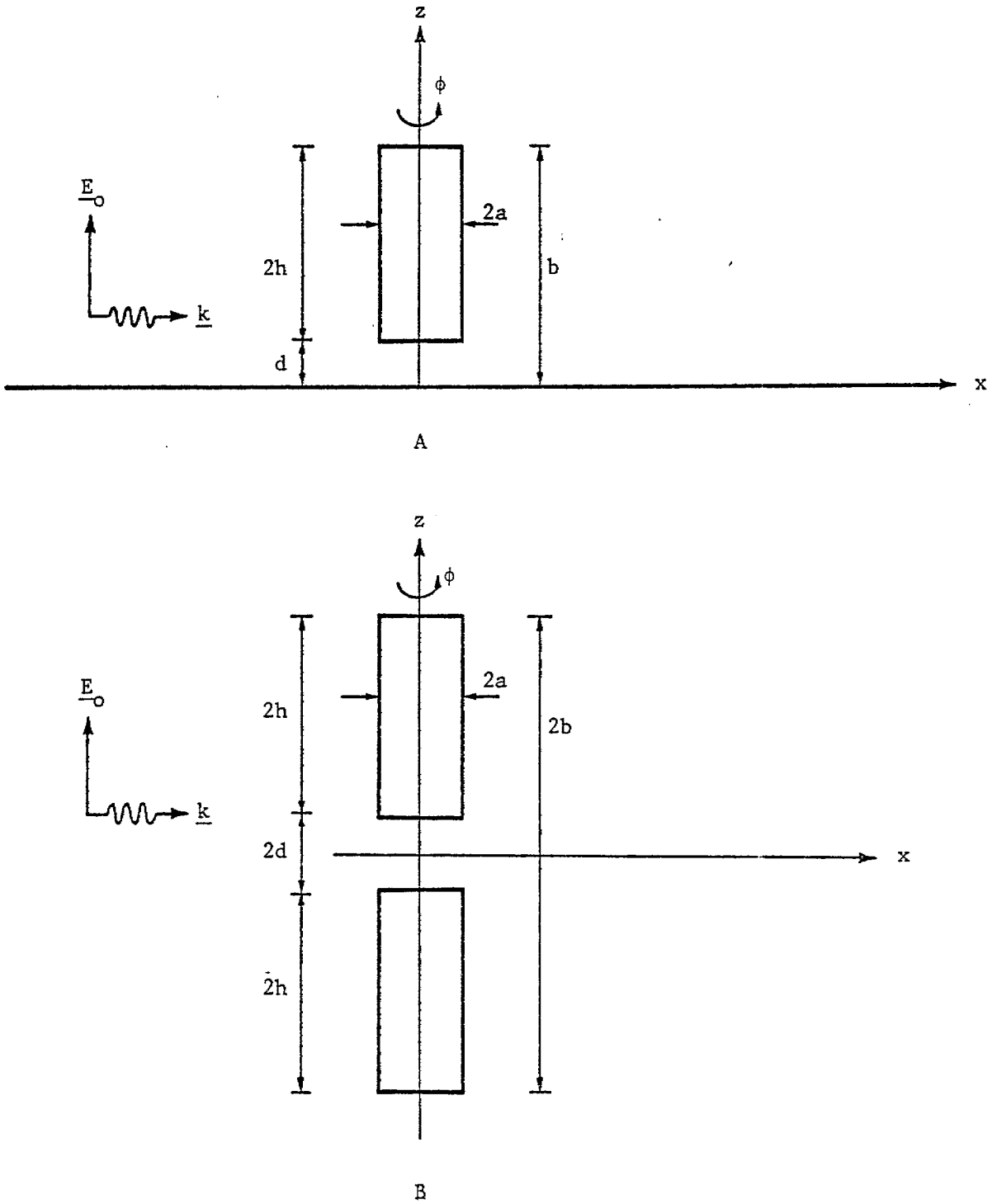


Figure 1. Electromagnetic interaction of one cylindrical post and a perfectly conducting plane (A) and electromagnetic interaction of two cylindrical posts (B): two equivalent situations.

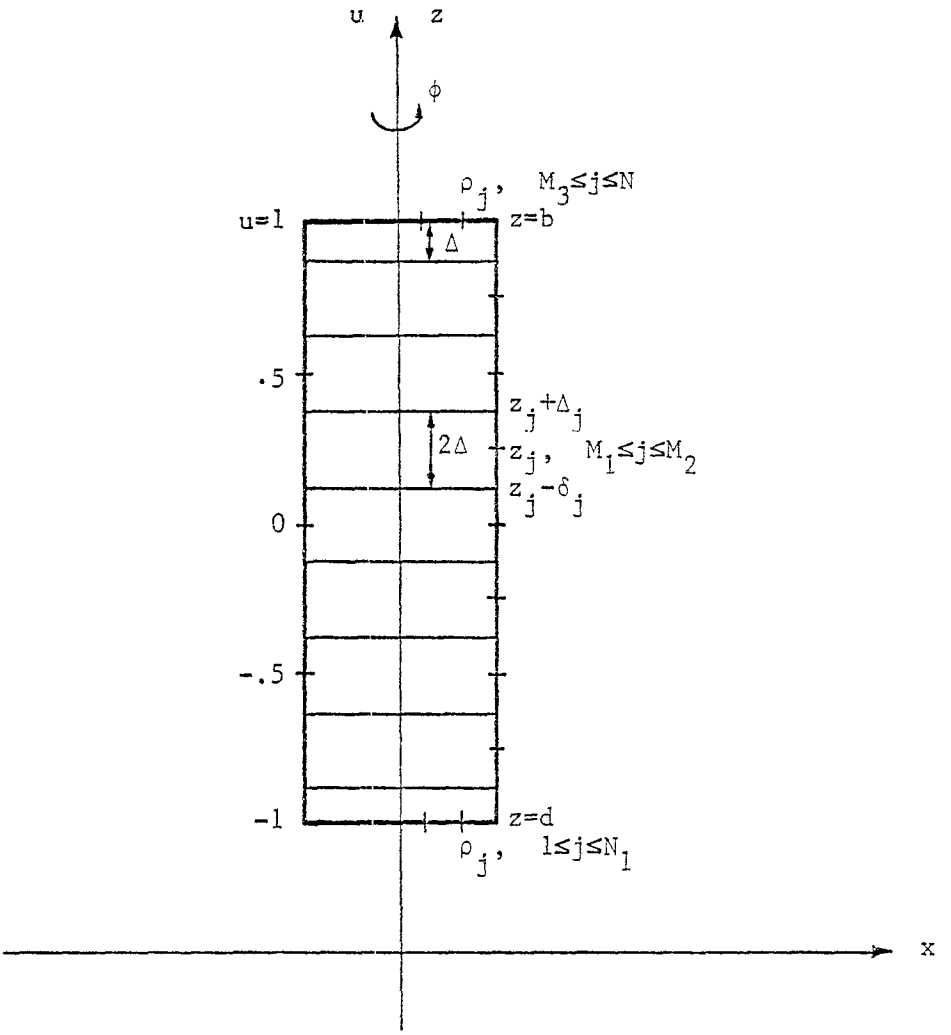


Figure 2. The zones and sample points used in the numerical quadrature of the integral equation.

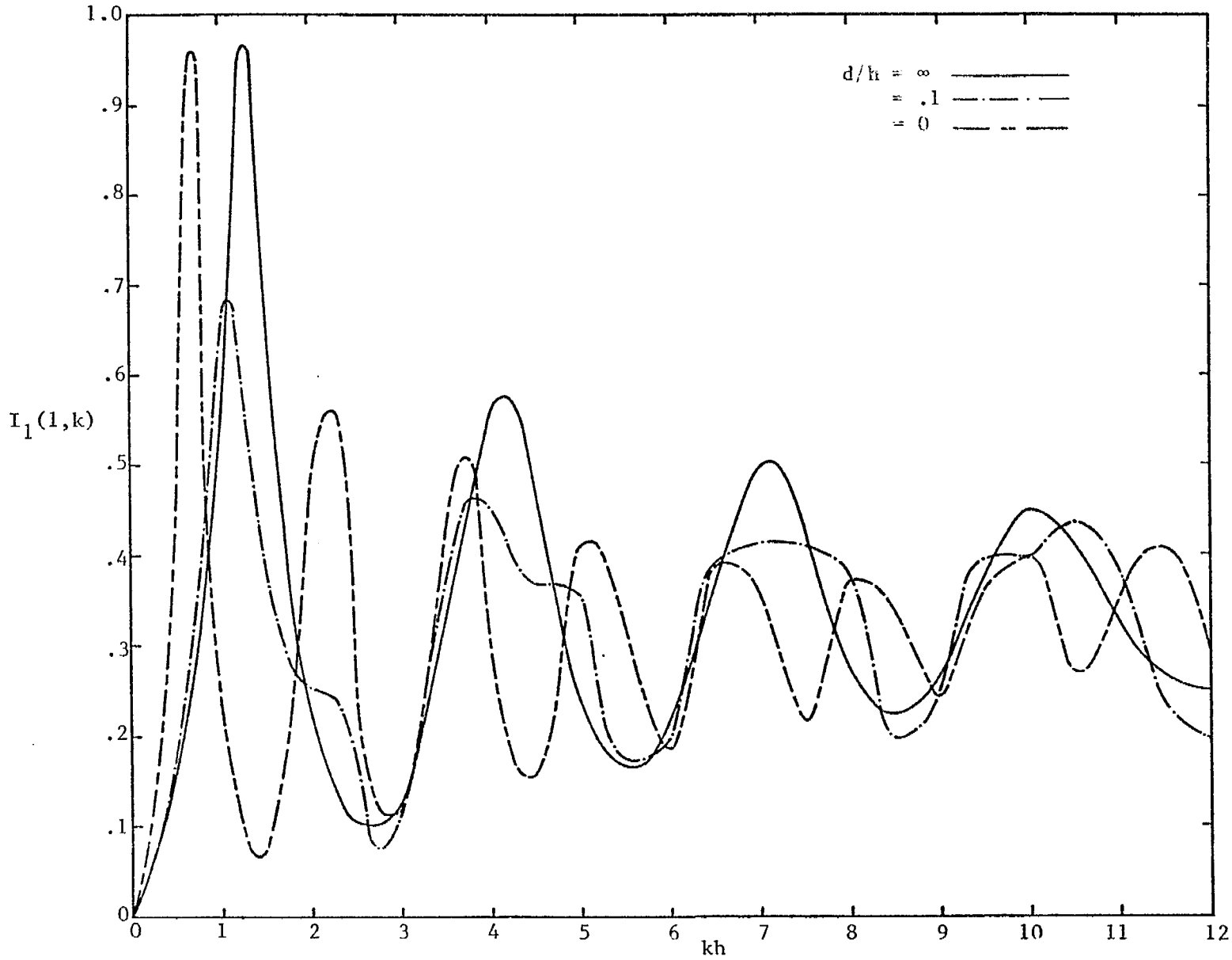


Figure 3a. Post current at u=1 versus frequency.

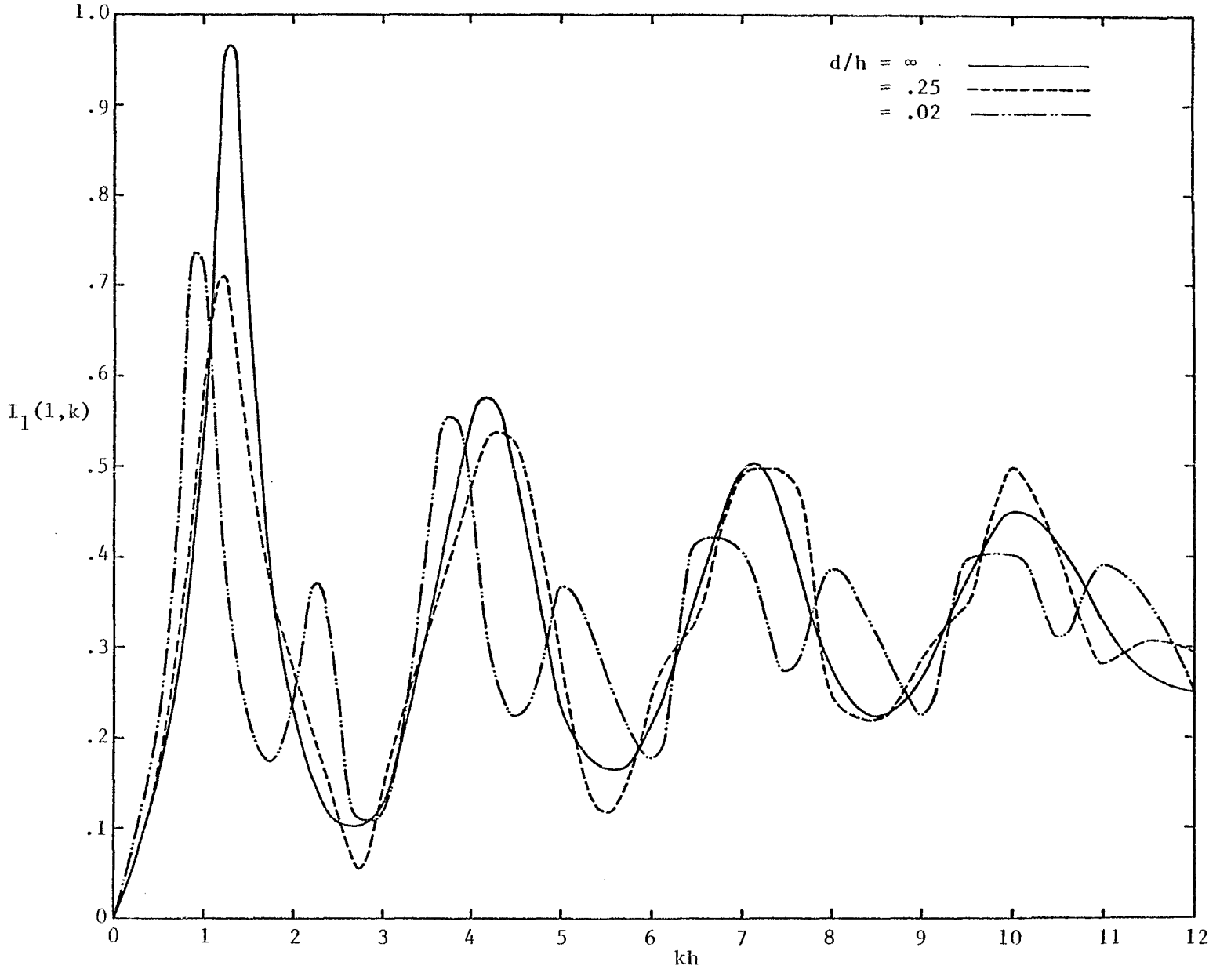


Figure 3b. Post current at u=1 versus frequency.

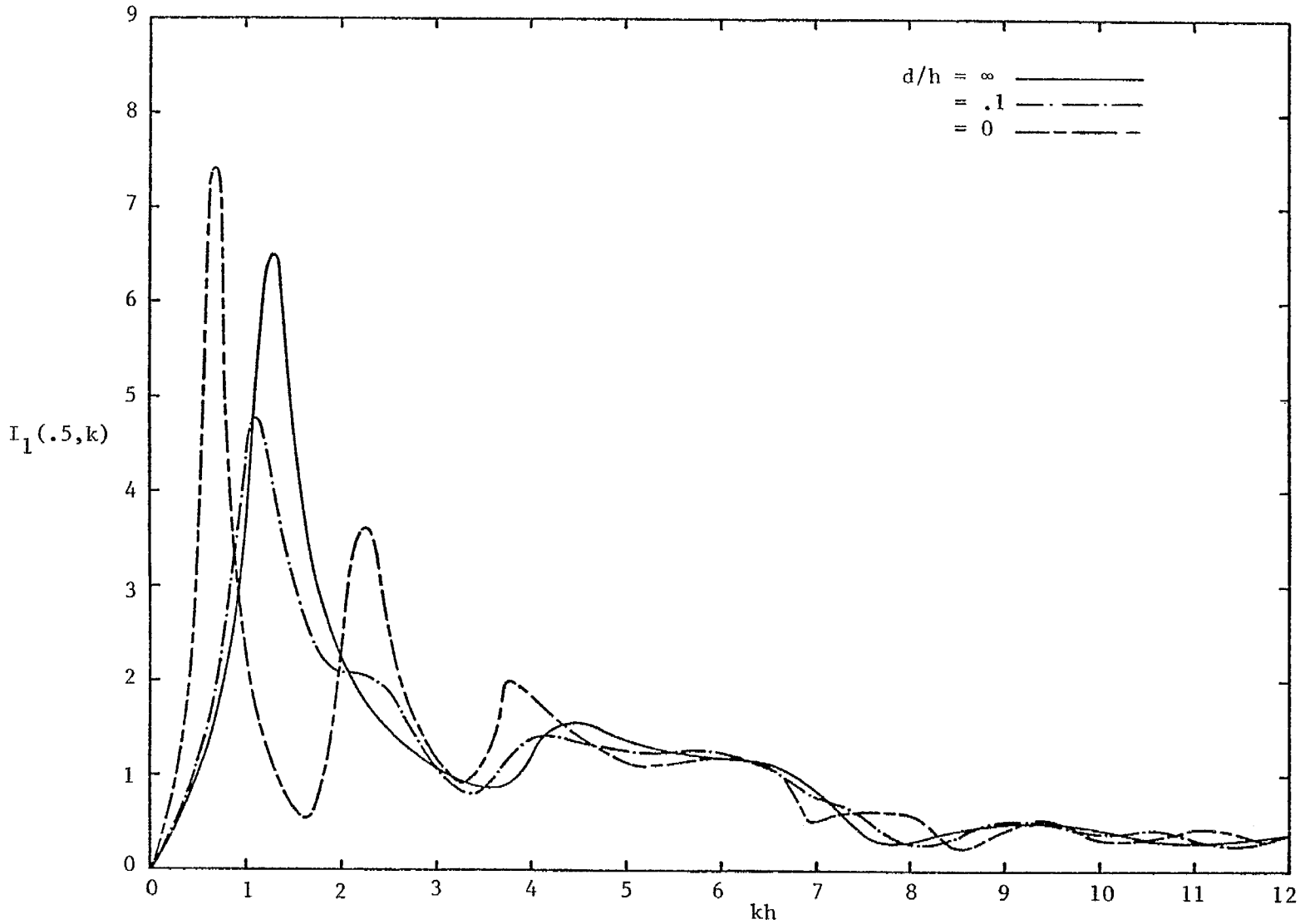


Figure 4a. Post current at u=.5 versus frequency.

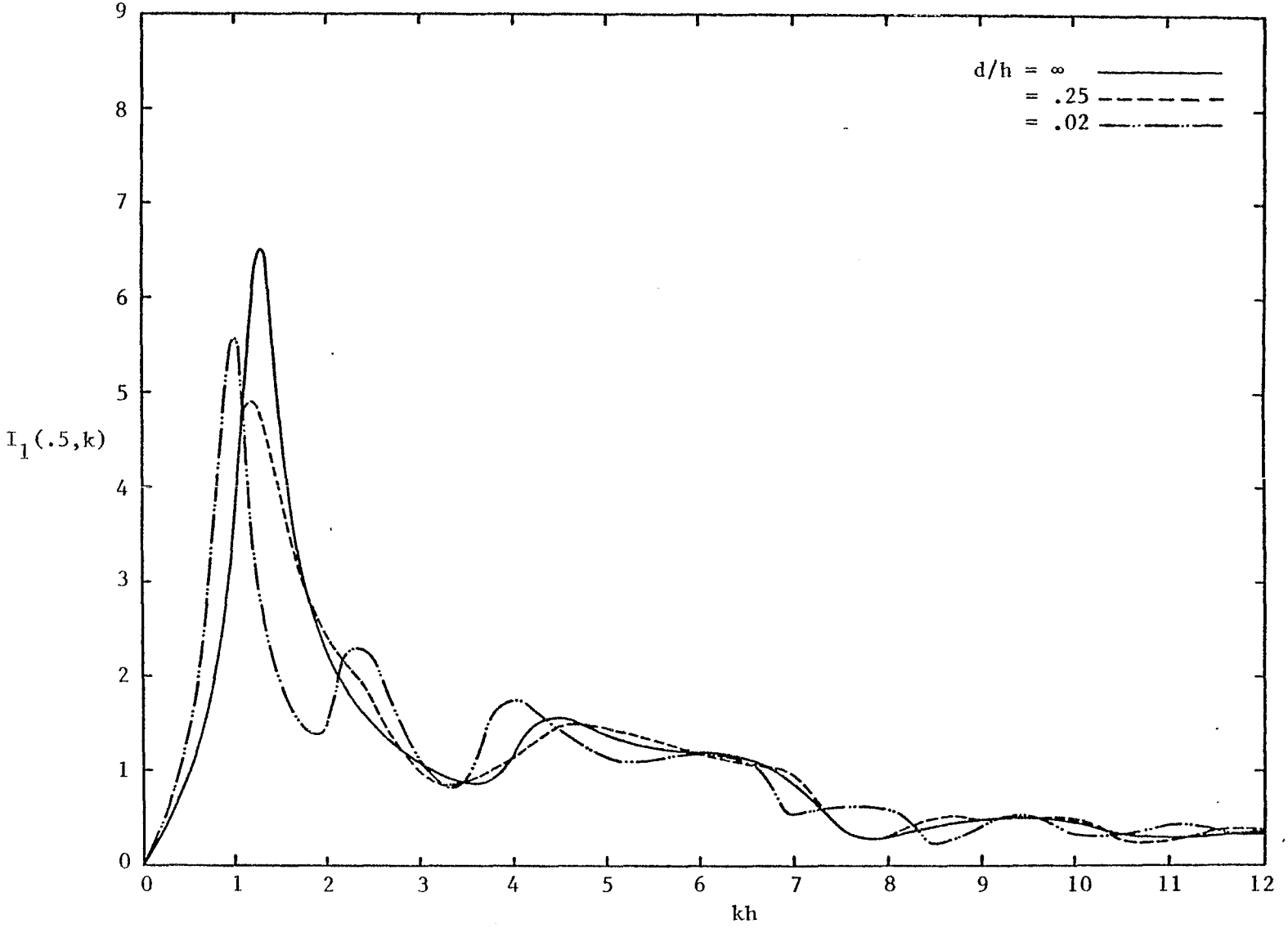


Figure 4b. Post current at u=.5 versus frequency.

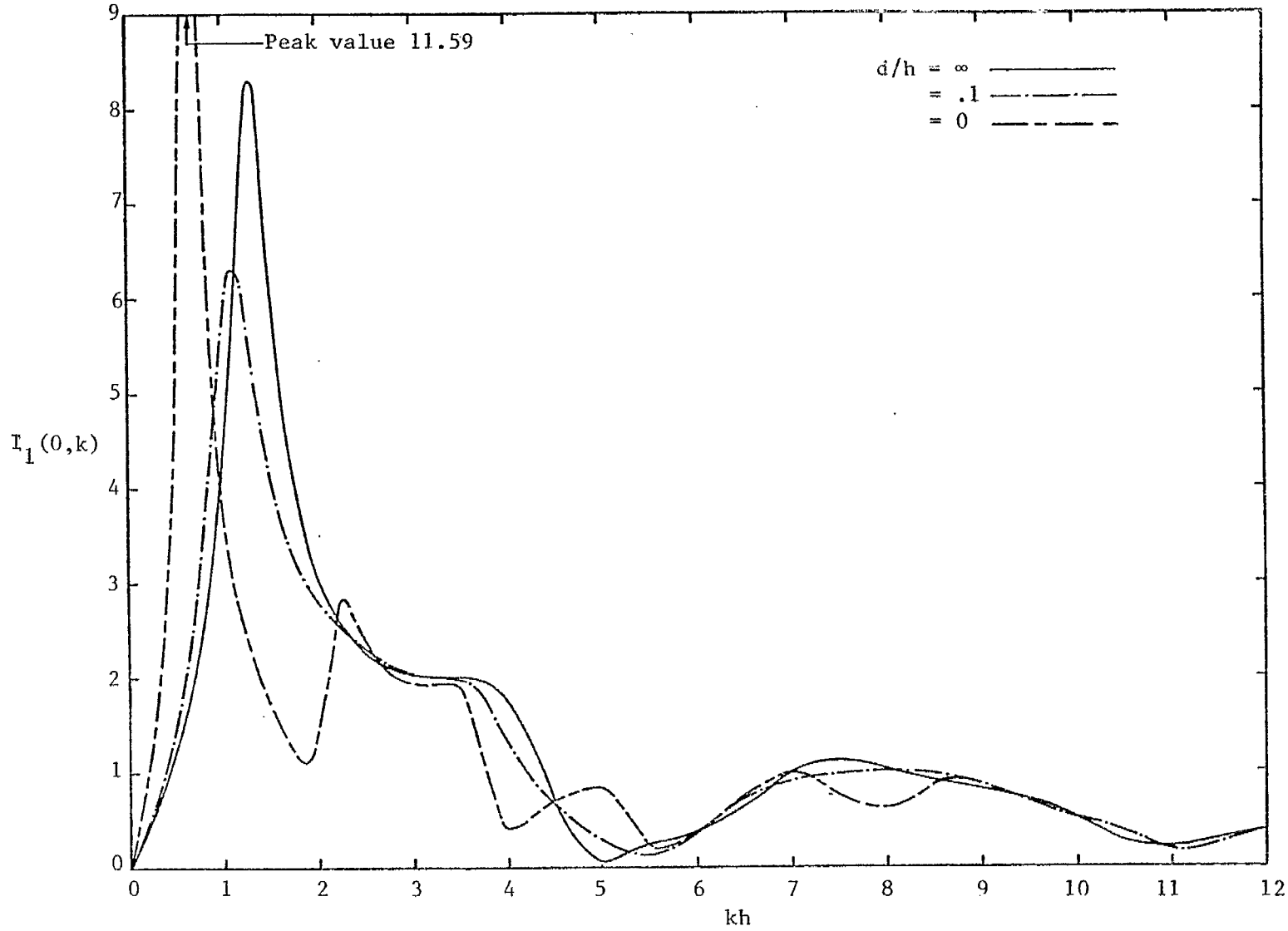


Figure 5a. Post current at u=0 versus frequency.

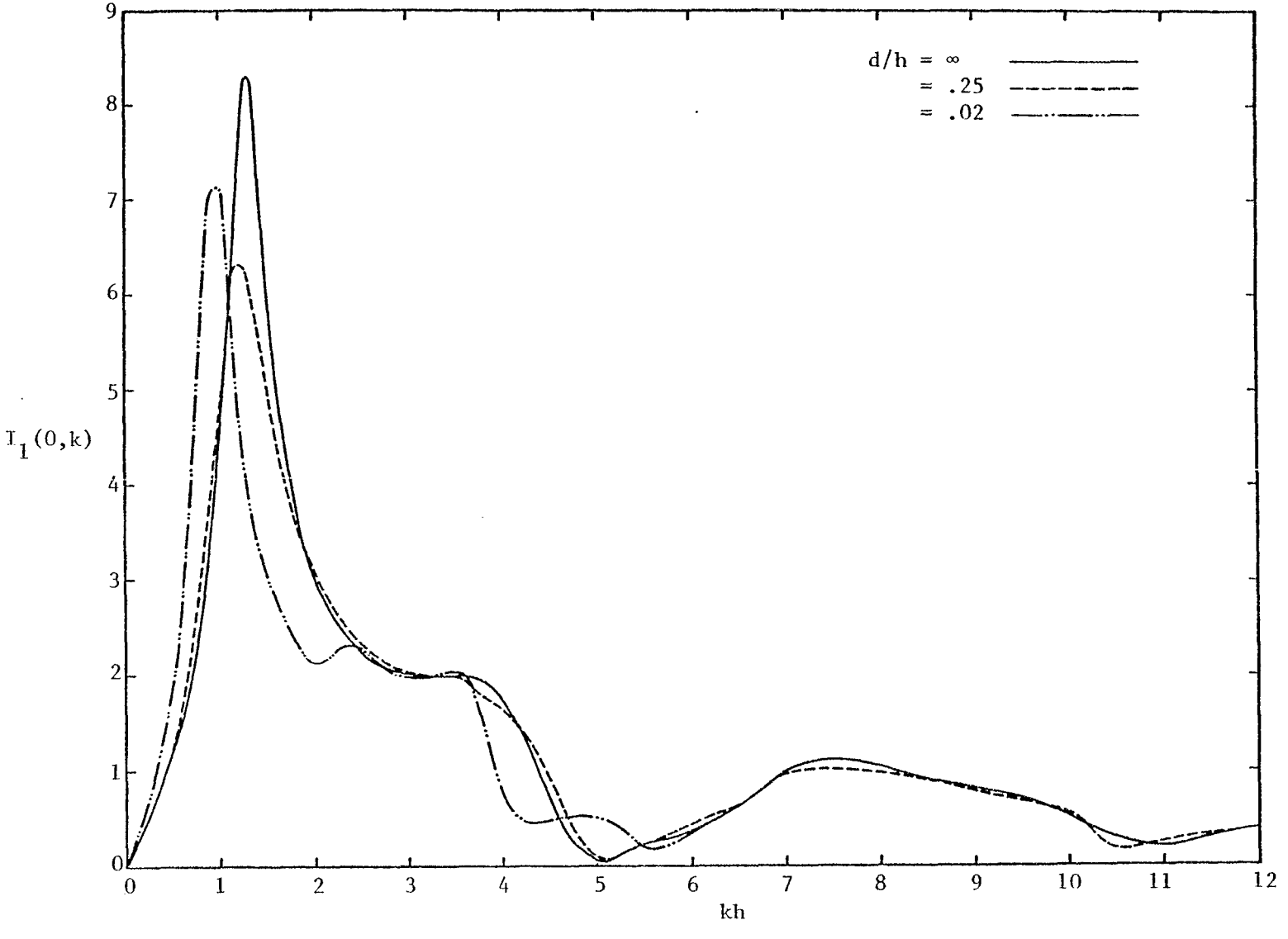


Figure 5b. Post current at u=0 versus frequency.

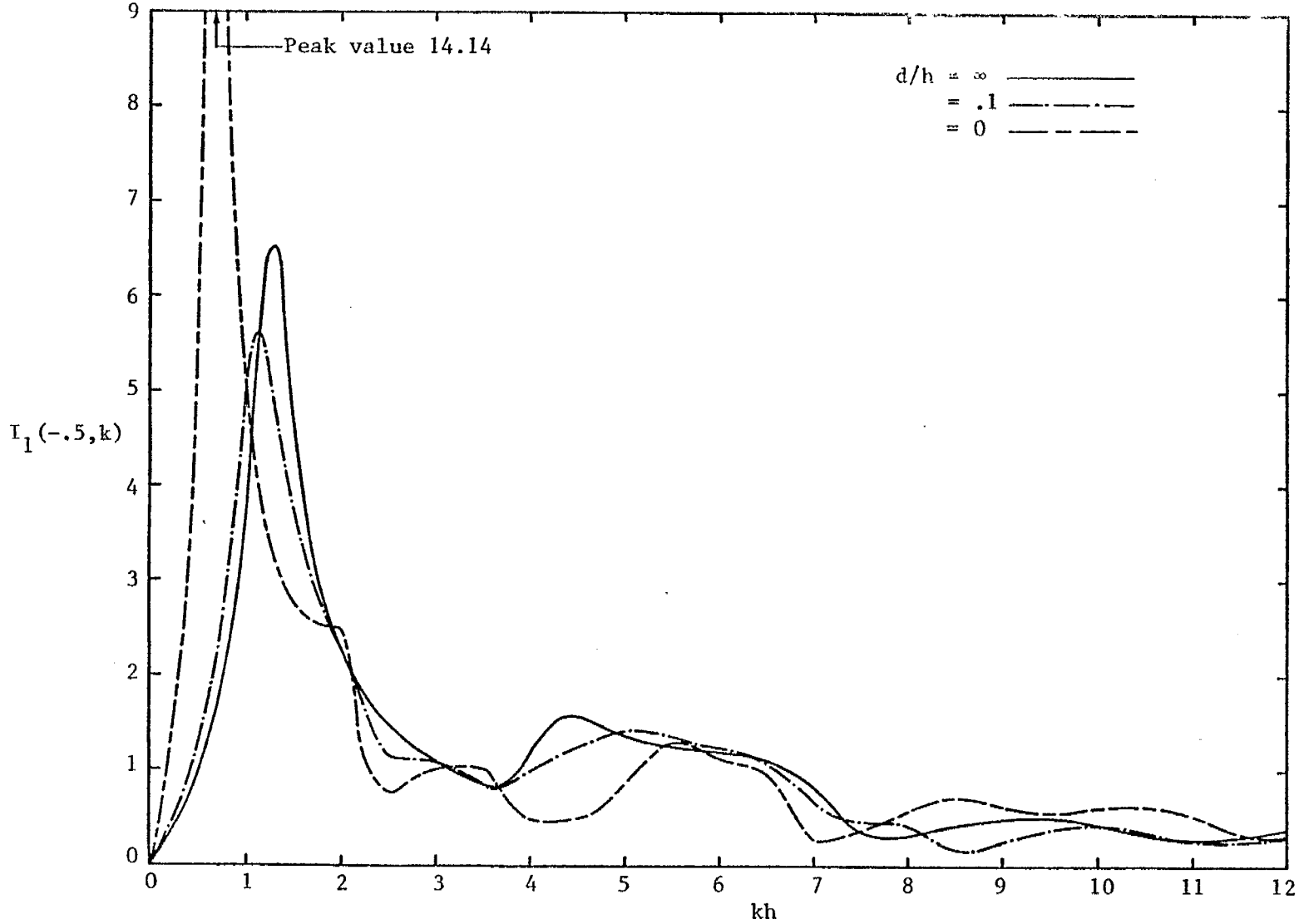


Figure 6a. Post current at u=-.5 versus frequency.

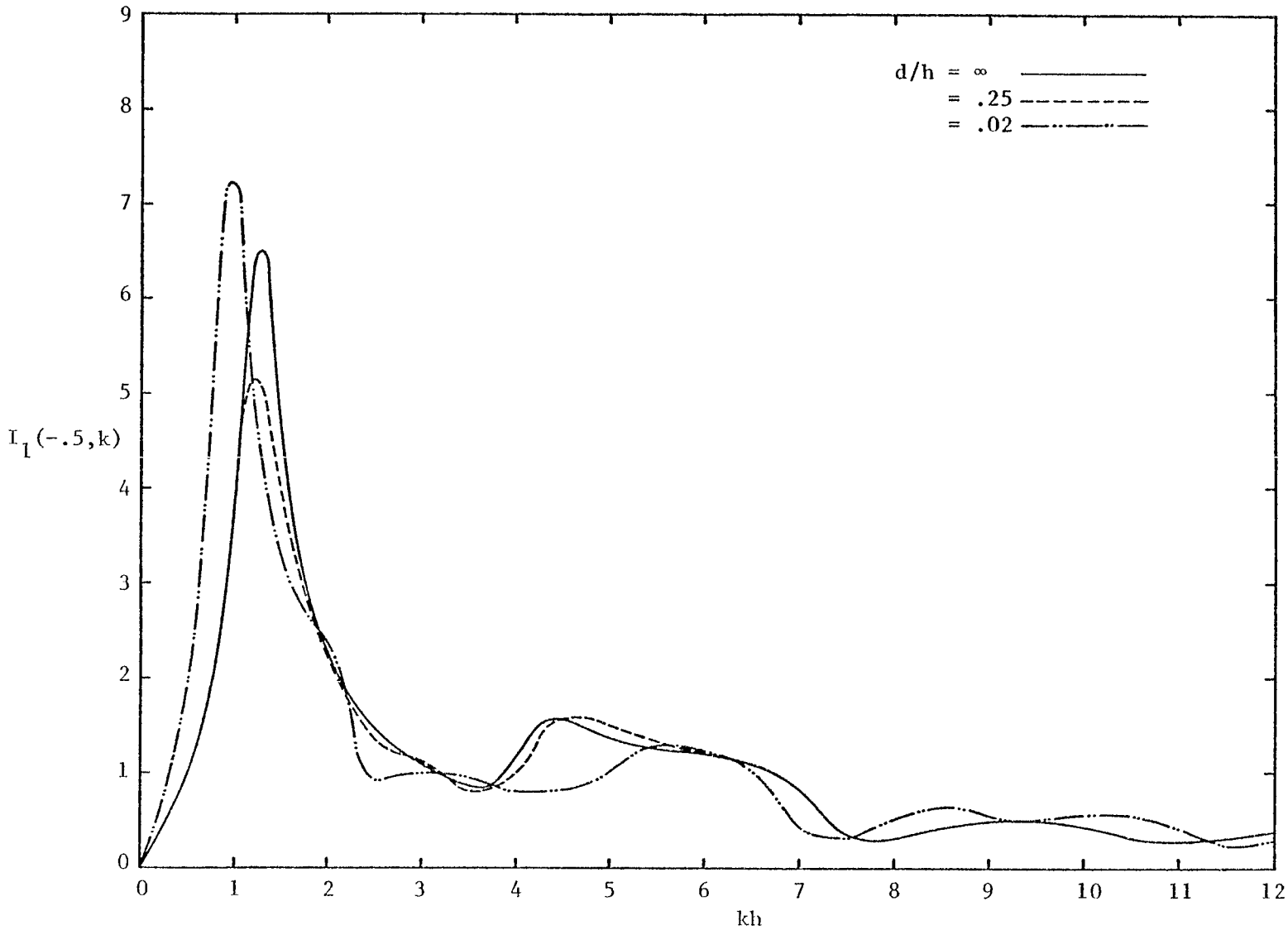


Figure 6b. Post current at u=-.5 versus frequency.

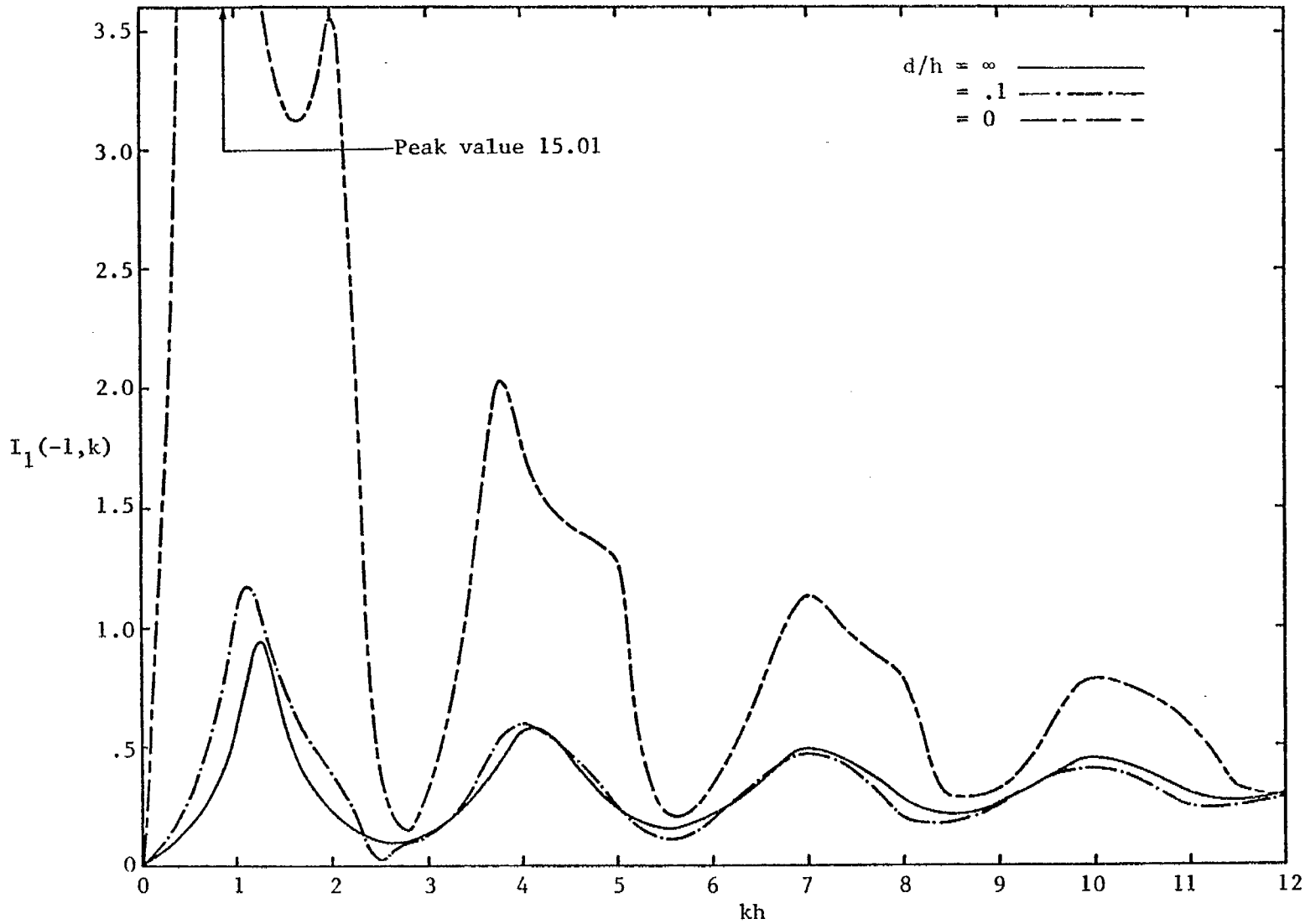


Figure 7a. Post current at u=-1 versus frequency.

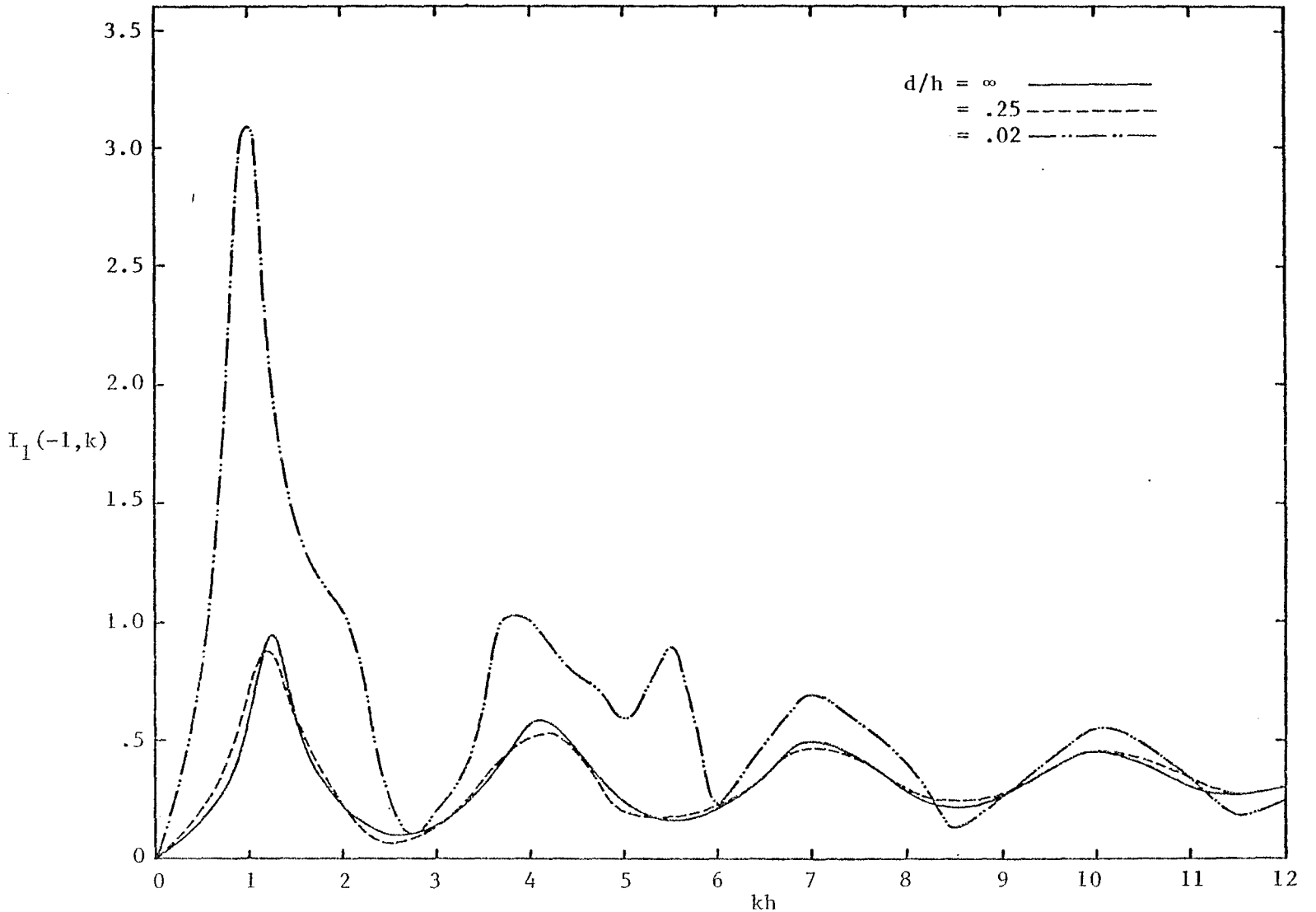


Figure 7b. Post current at u=-1 versus frequency.

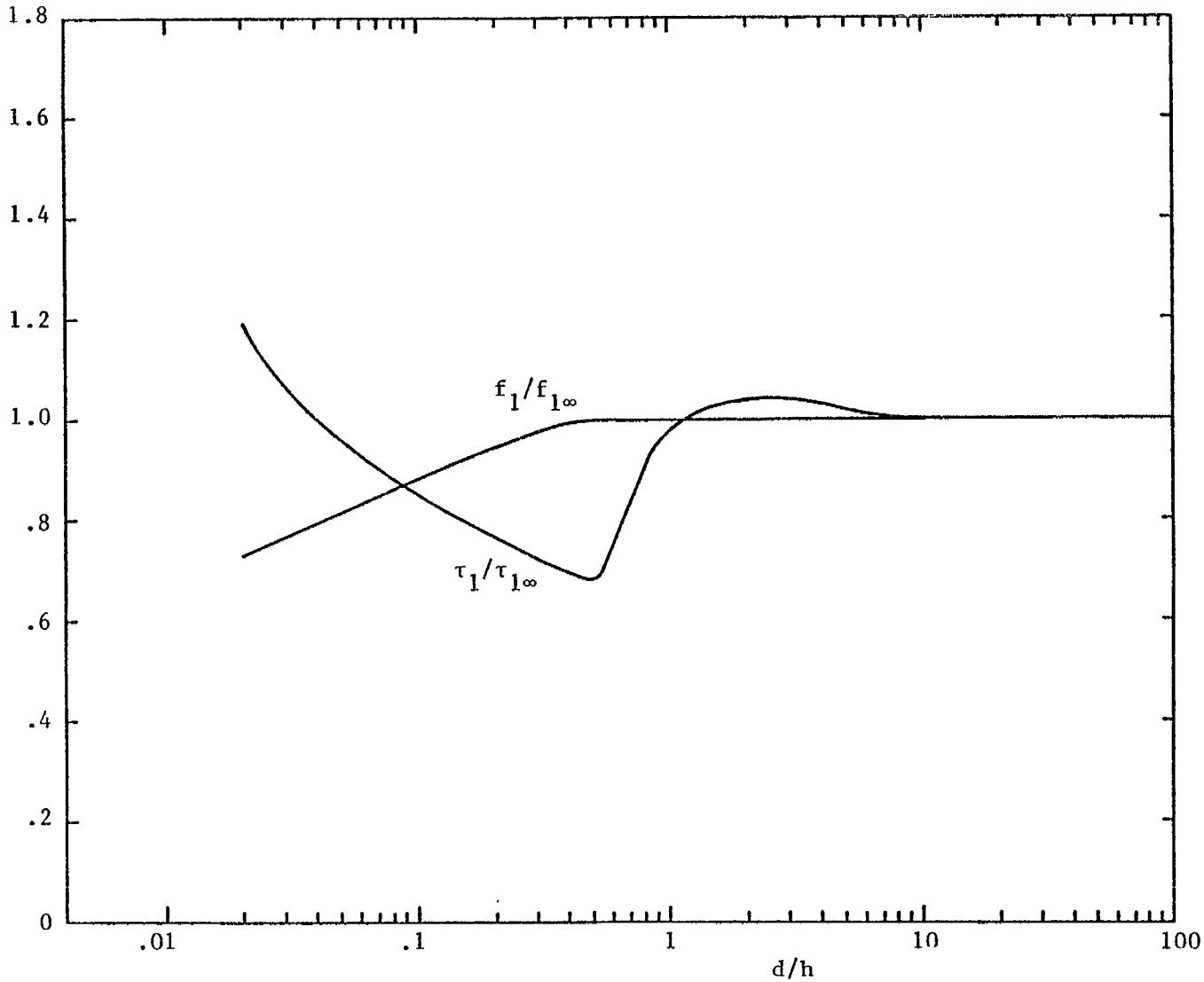


Figure 8. The variation with d/h of the resonant frequency and the decay constant of the dominant mode.

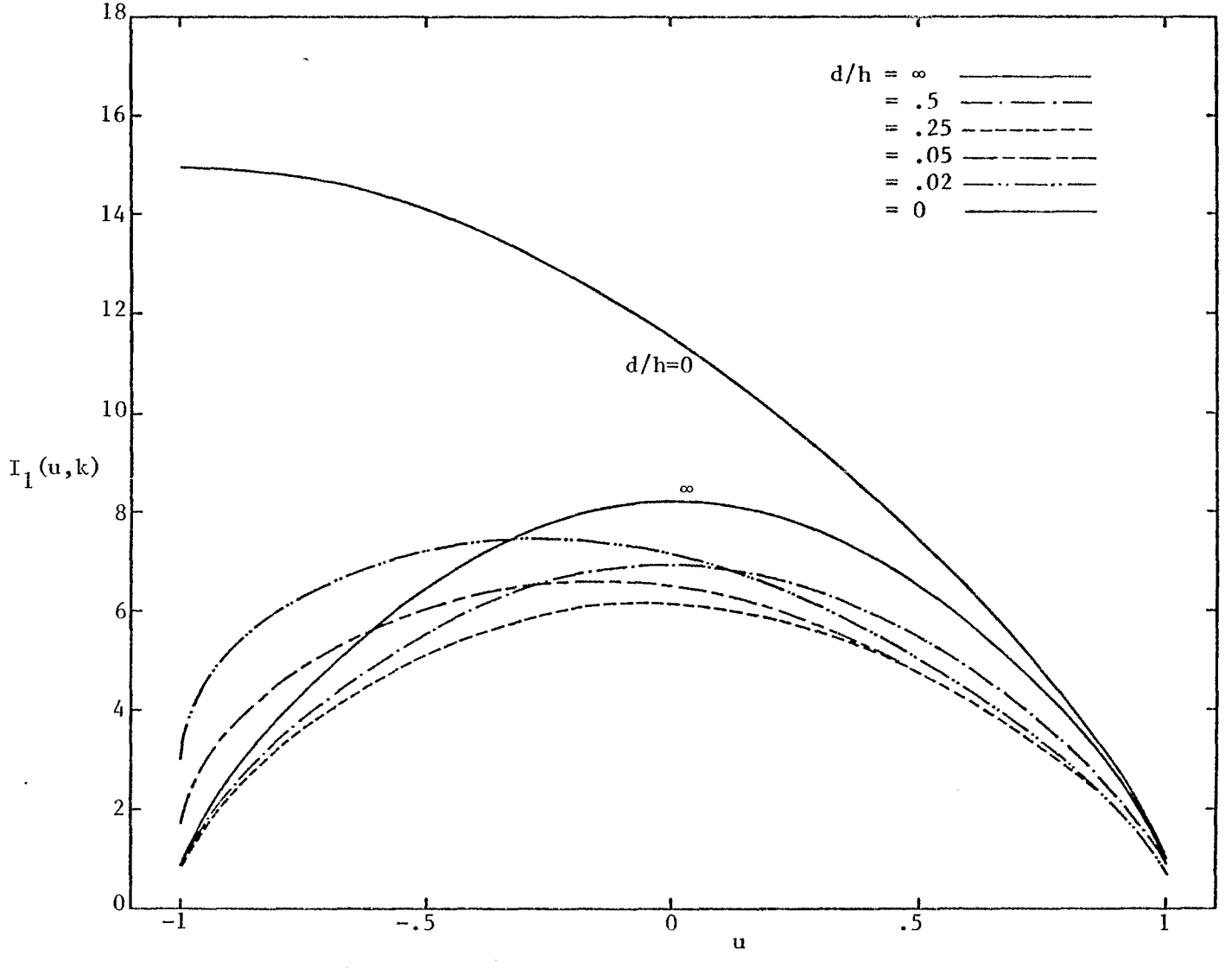


Figure 9. Magnitude of current versus position at resonance frequency.

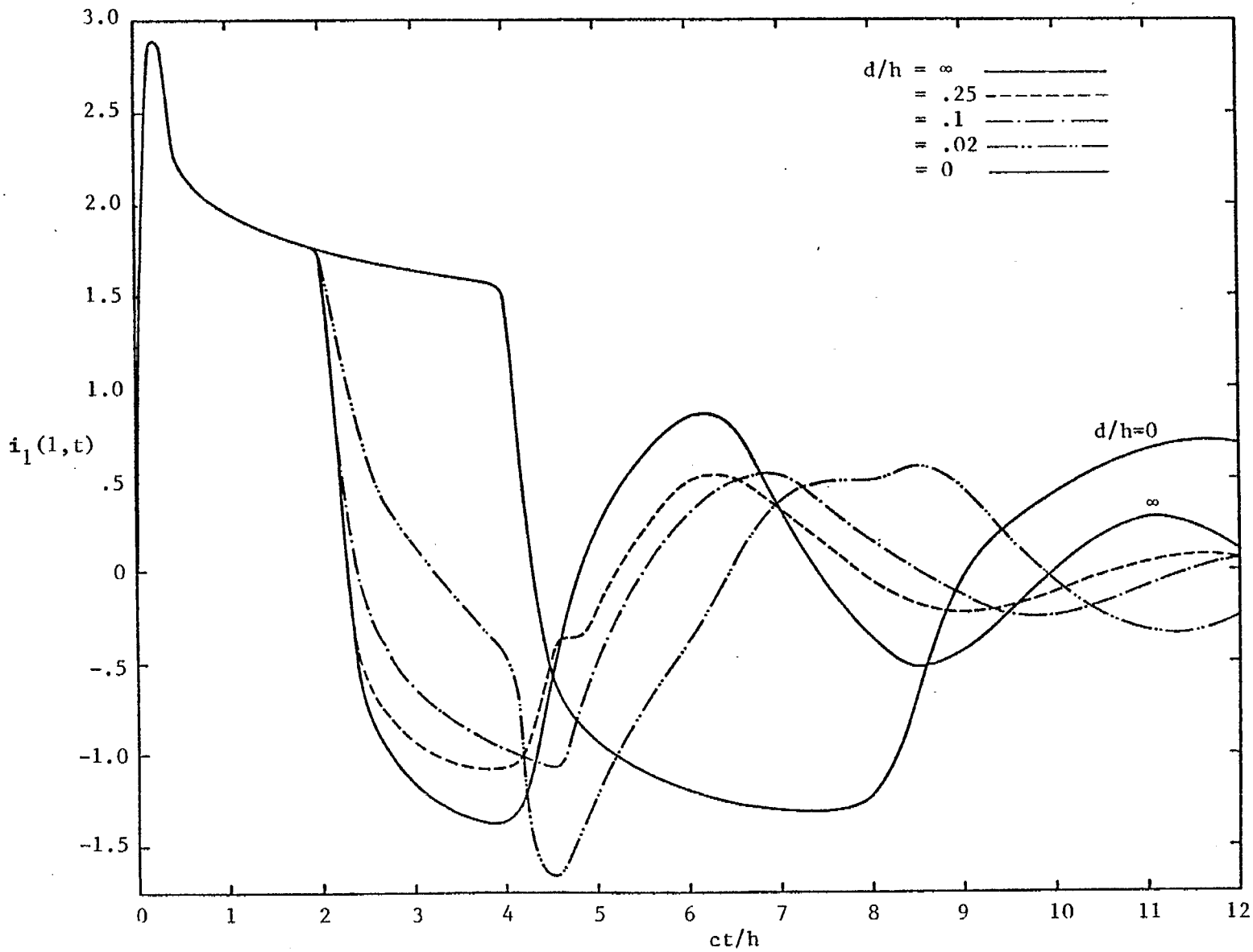


Figure 10. Post current at u=1 versus time.

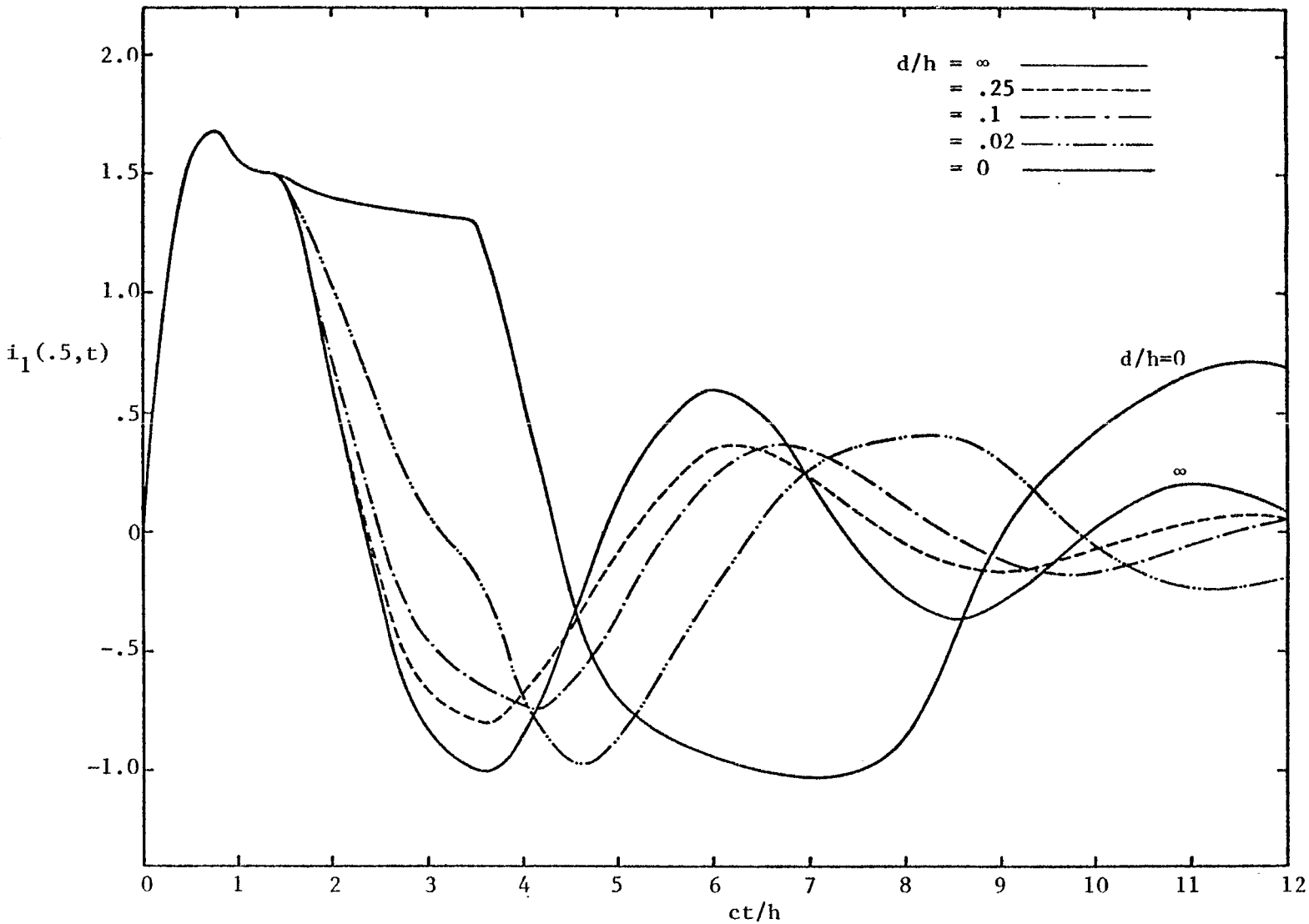


Figure 11. Post current at u=.5 versus time.

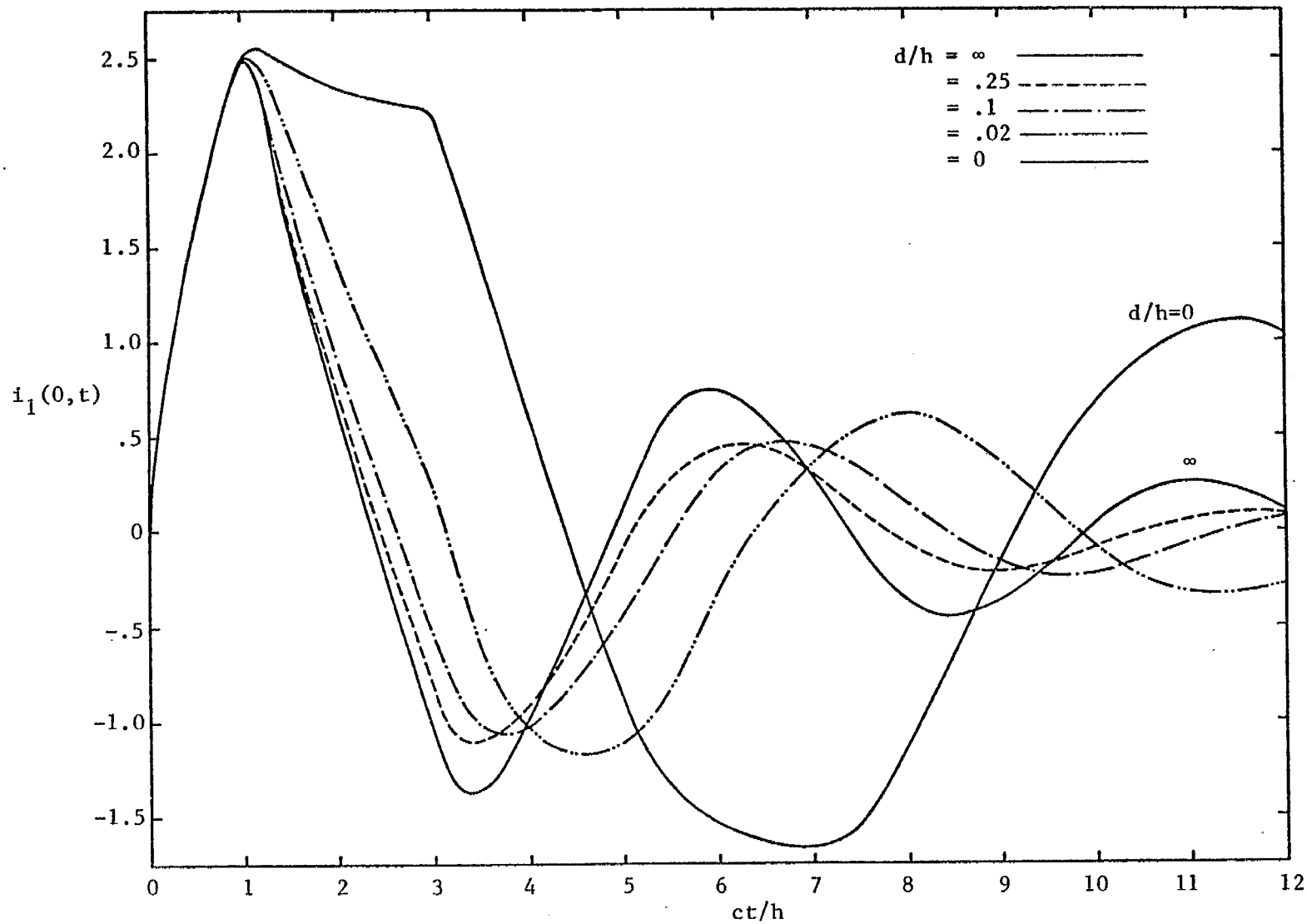


Figure 12. Post current at u=0 versus time.

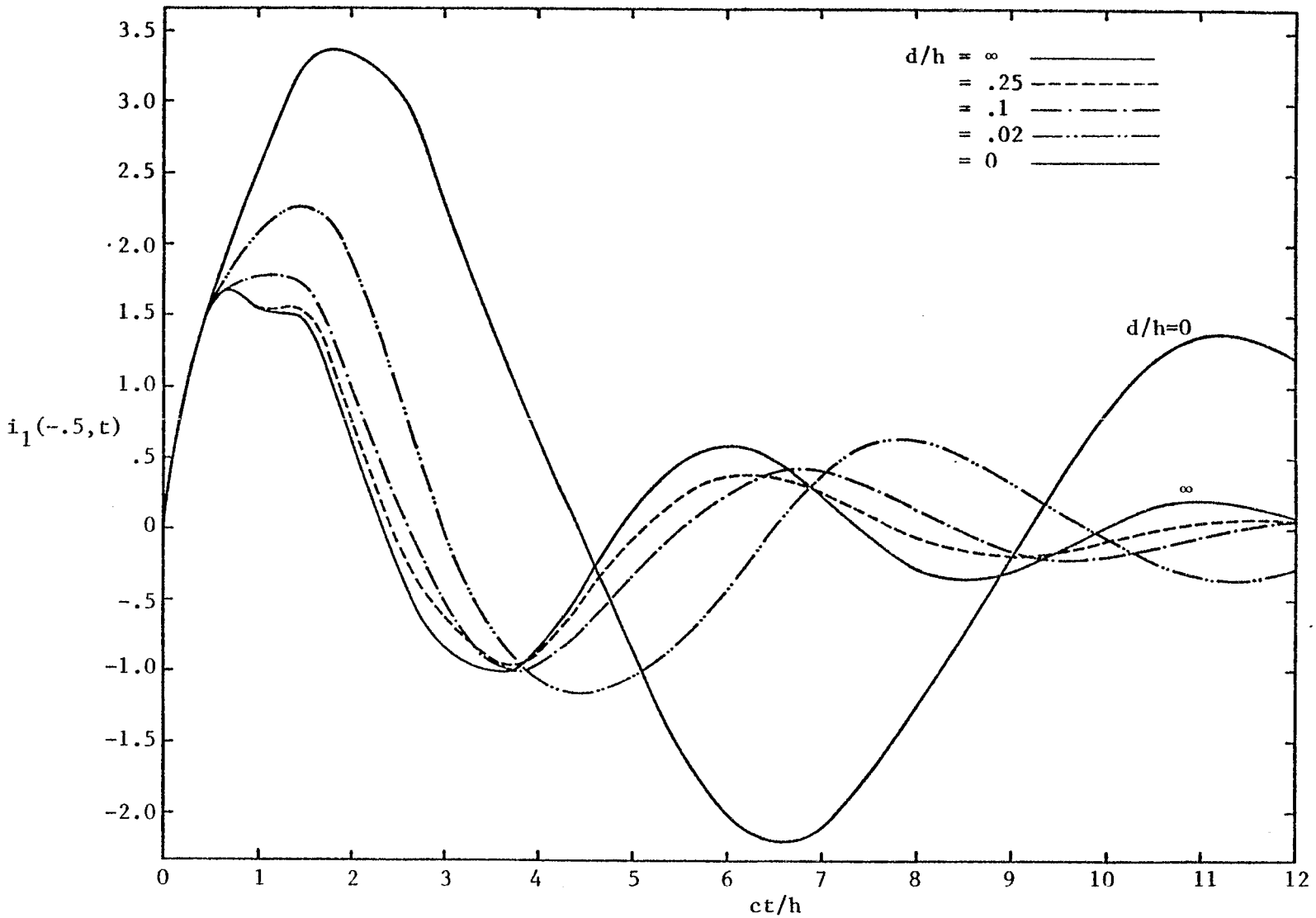


Figure 13. Post current at u=-.5 versus time.

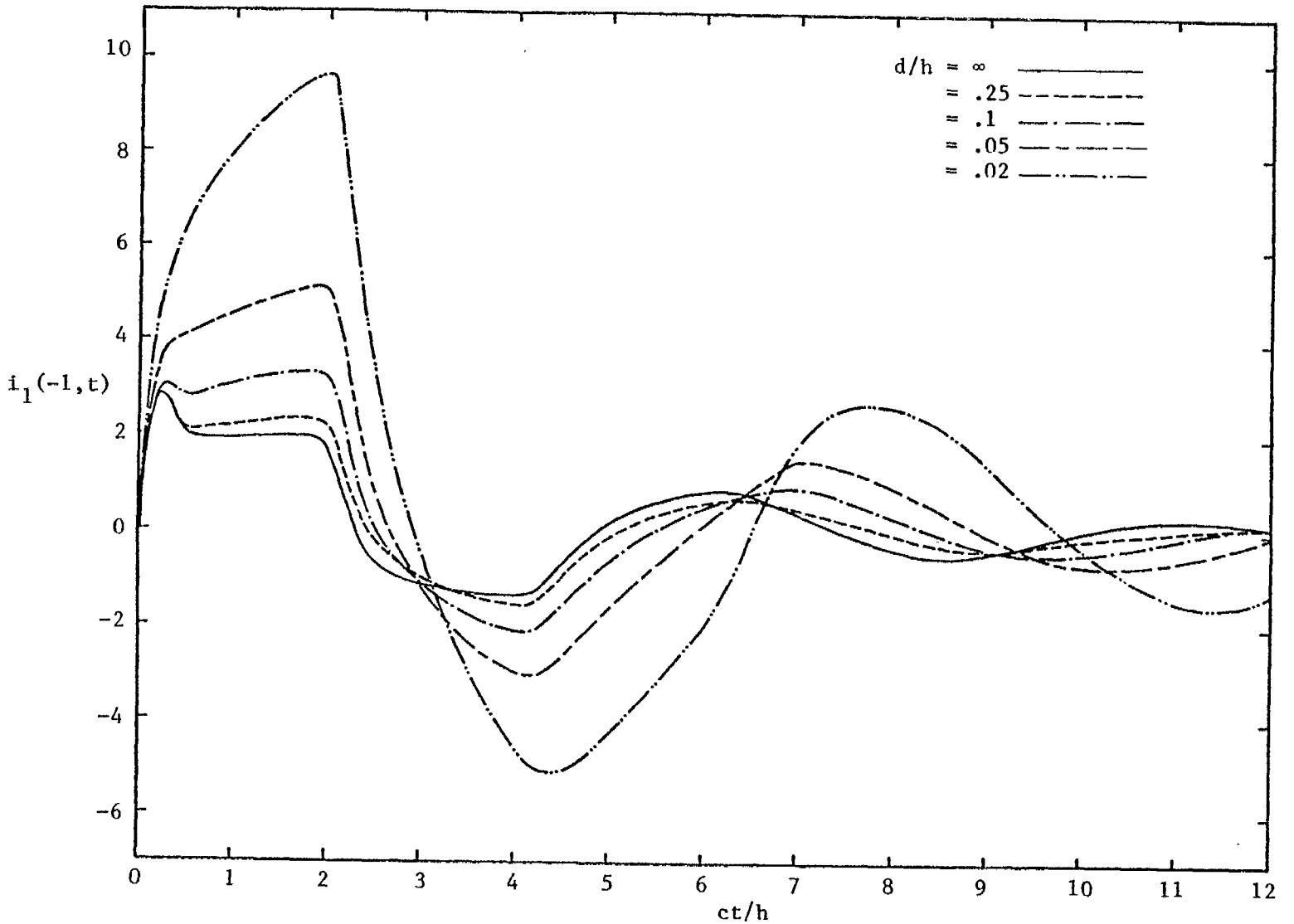


Figure 14. Post current at u=-1 versus time.

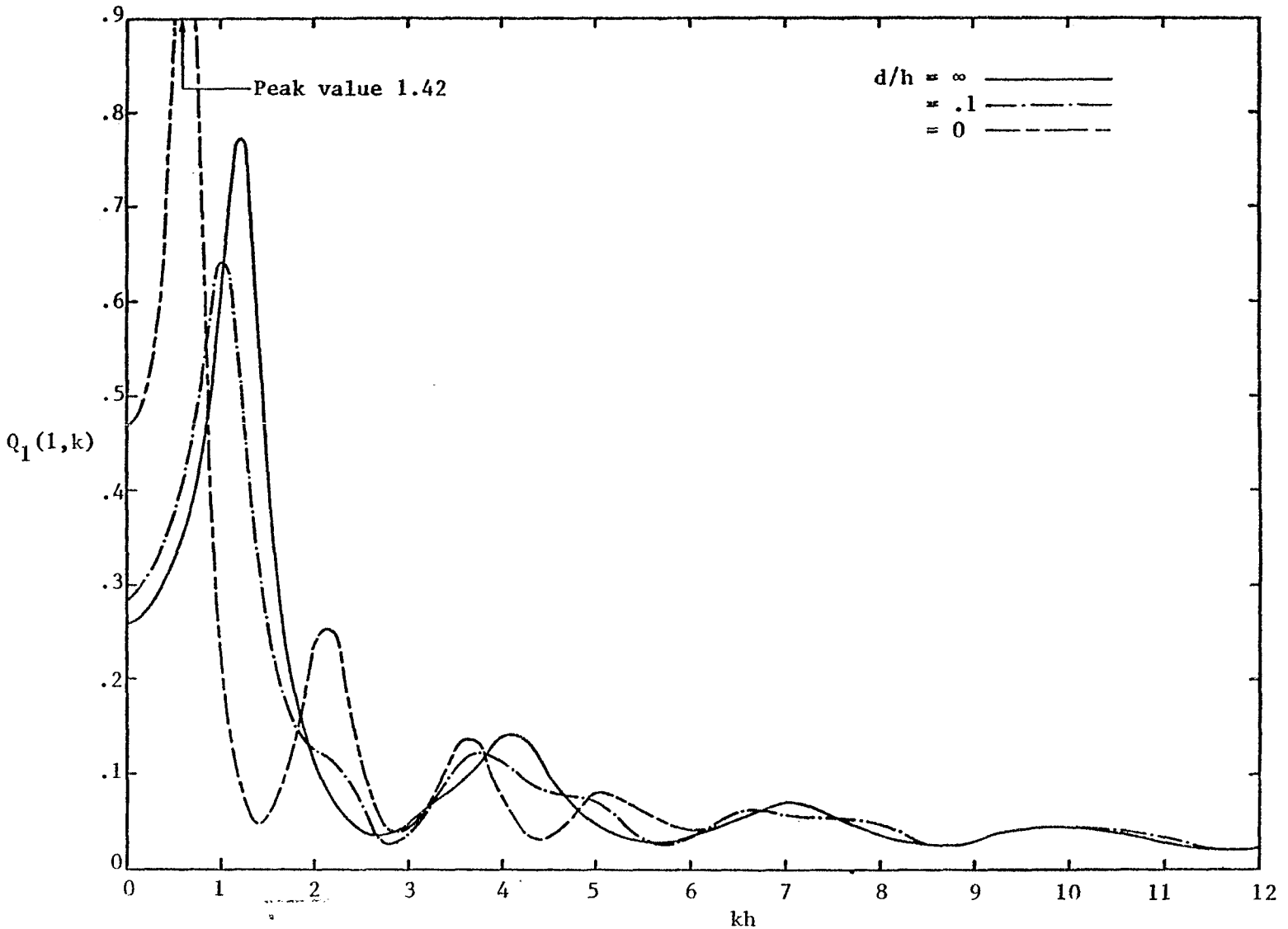


Figure 15a. The induced surface charge on the upper end of the post versus frequency.

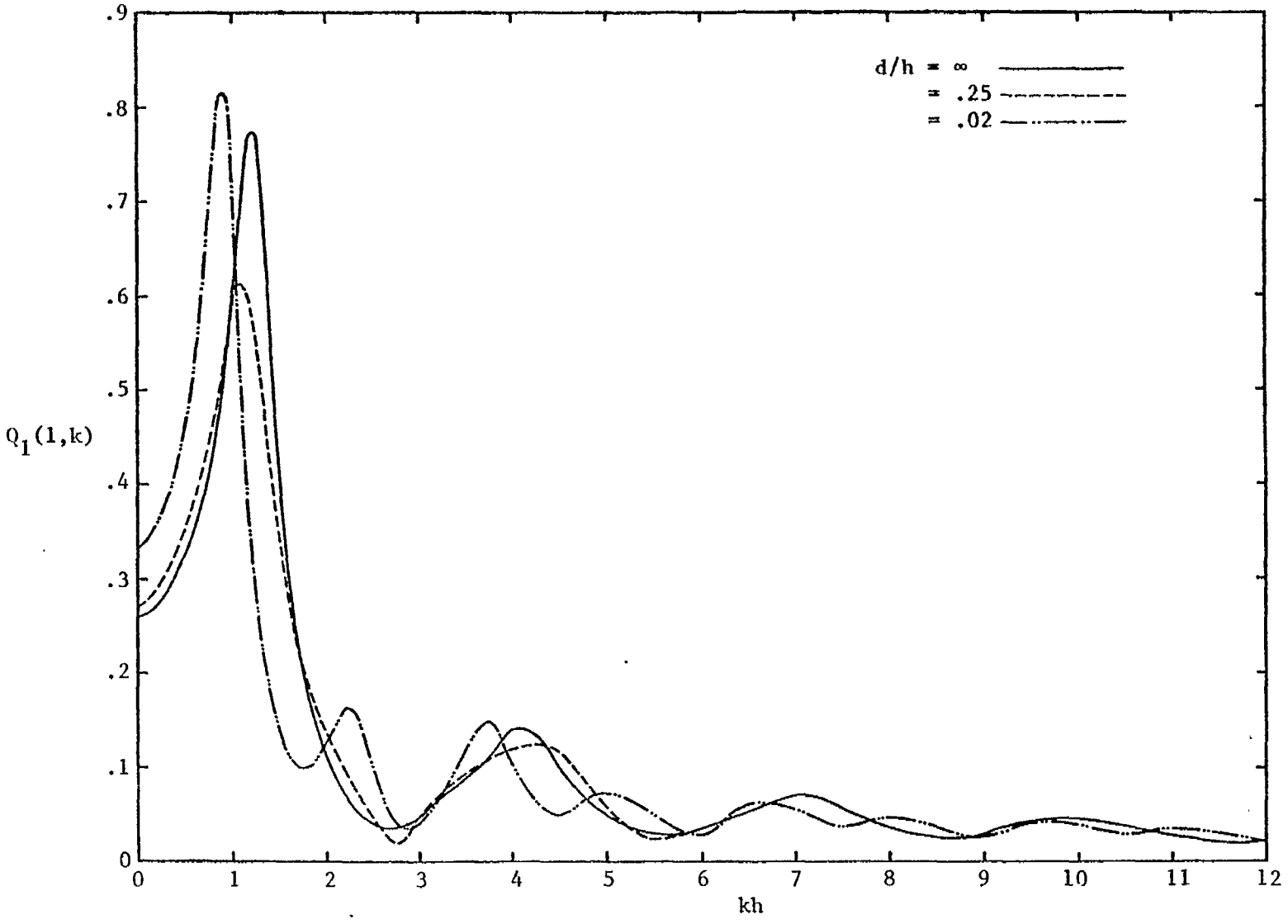


Figure 15b. The induced surface charge on the upper end of the post versus frequency.

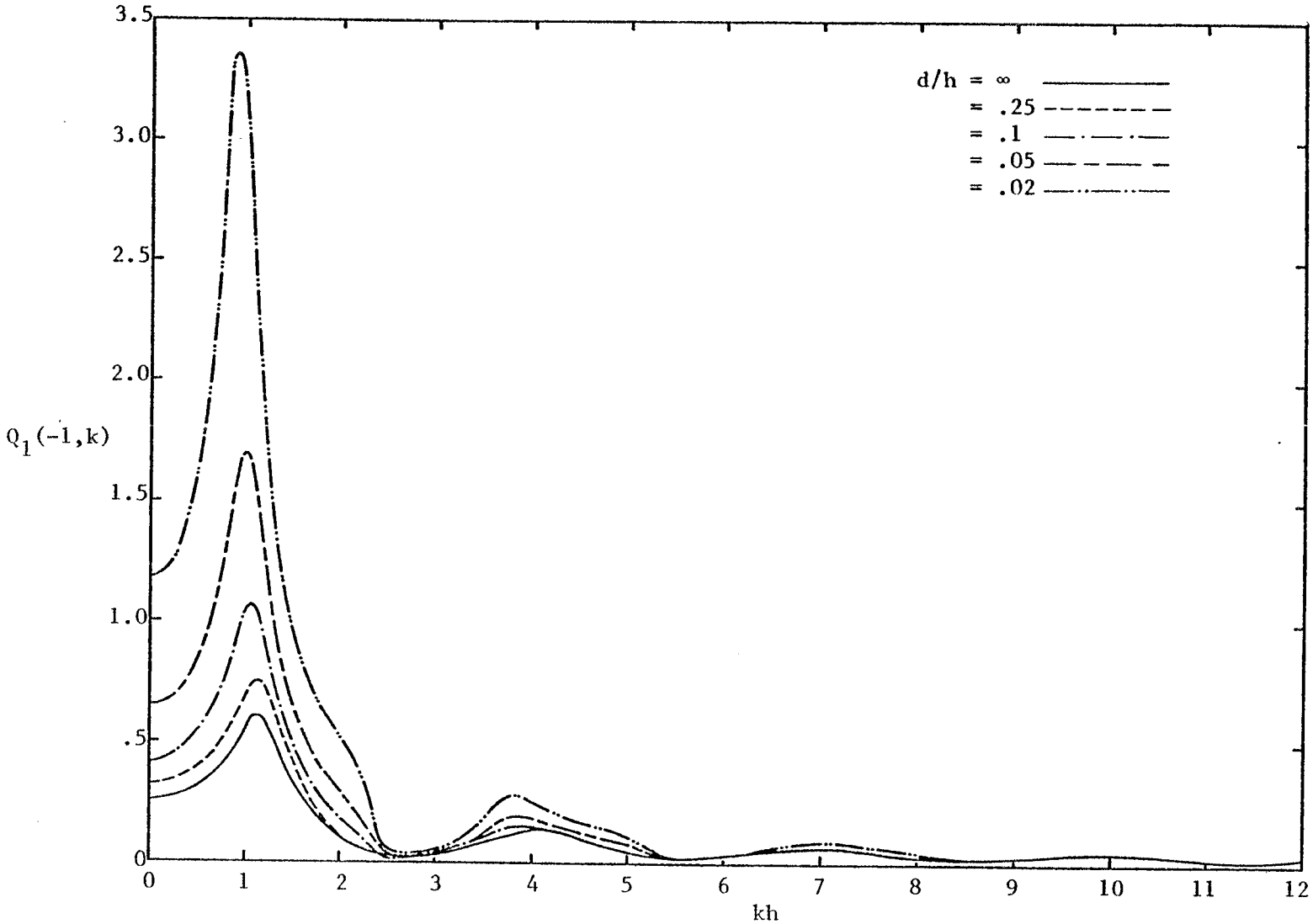


Figure 16. The induced surface charge on the lower end of the post versus frequency.

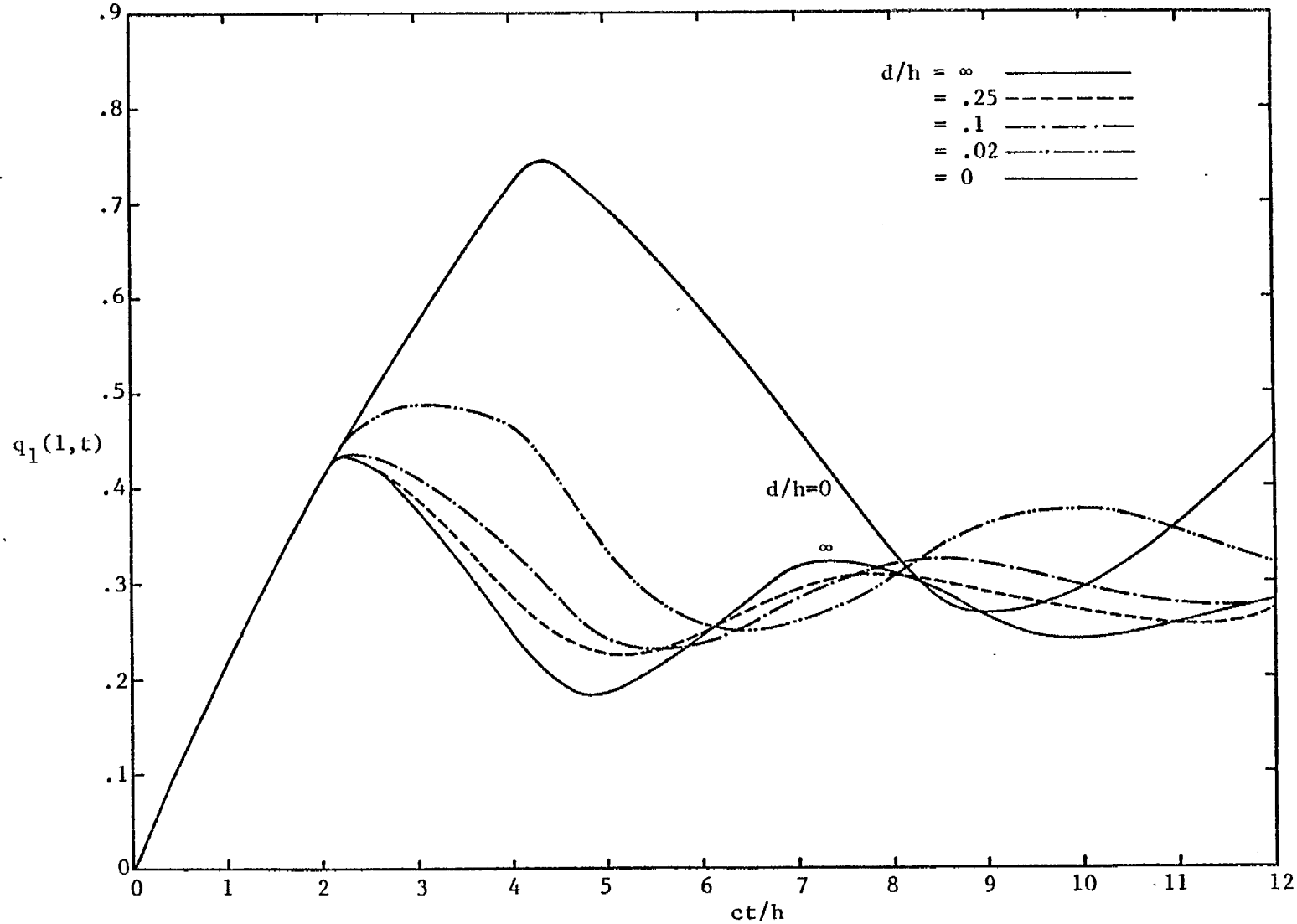


Figure 17. The induced surface charge on the upper end of the post versus time.

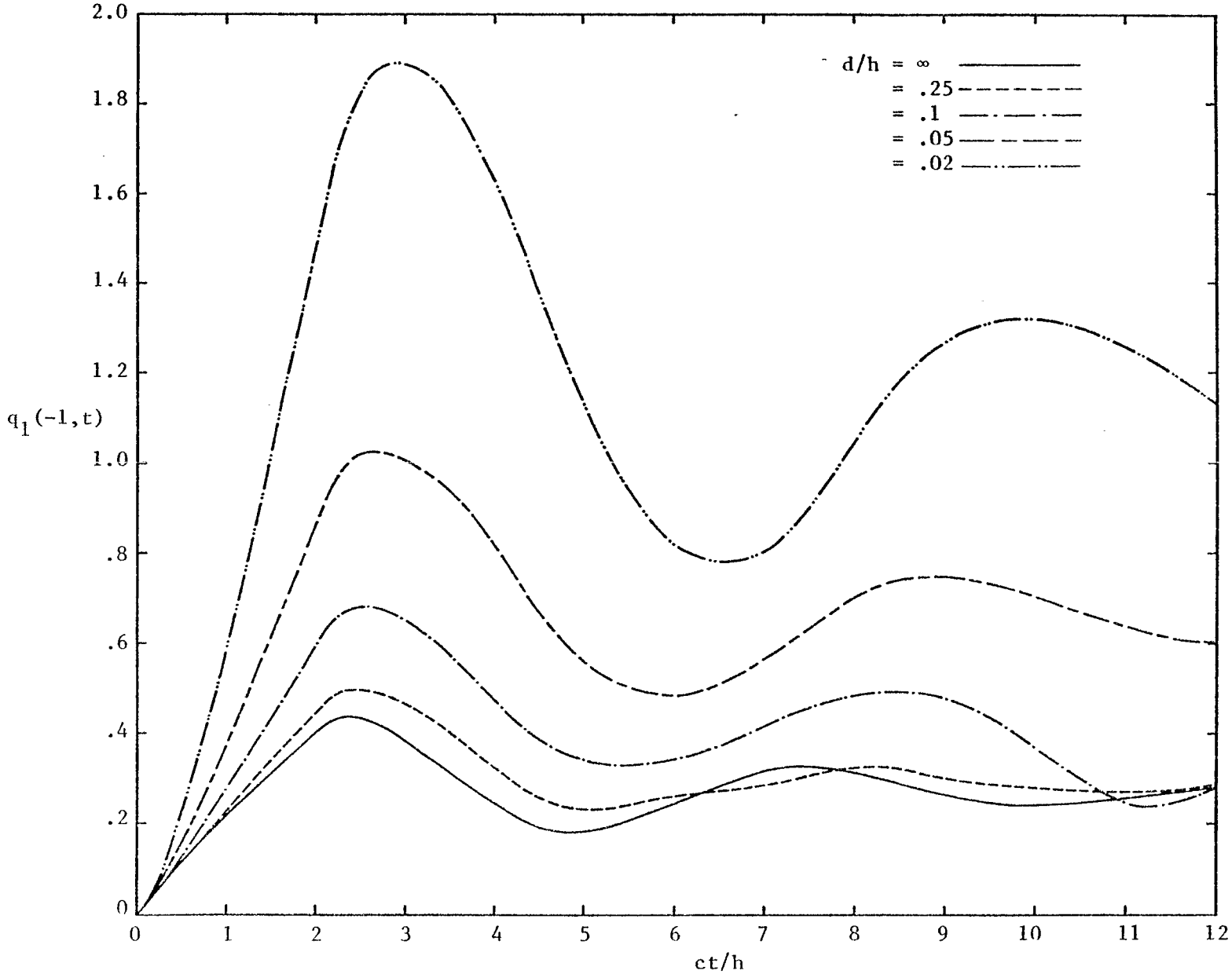


Figure 18. The induced surface charge on the lower end of the post versus time.

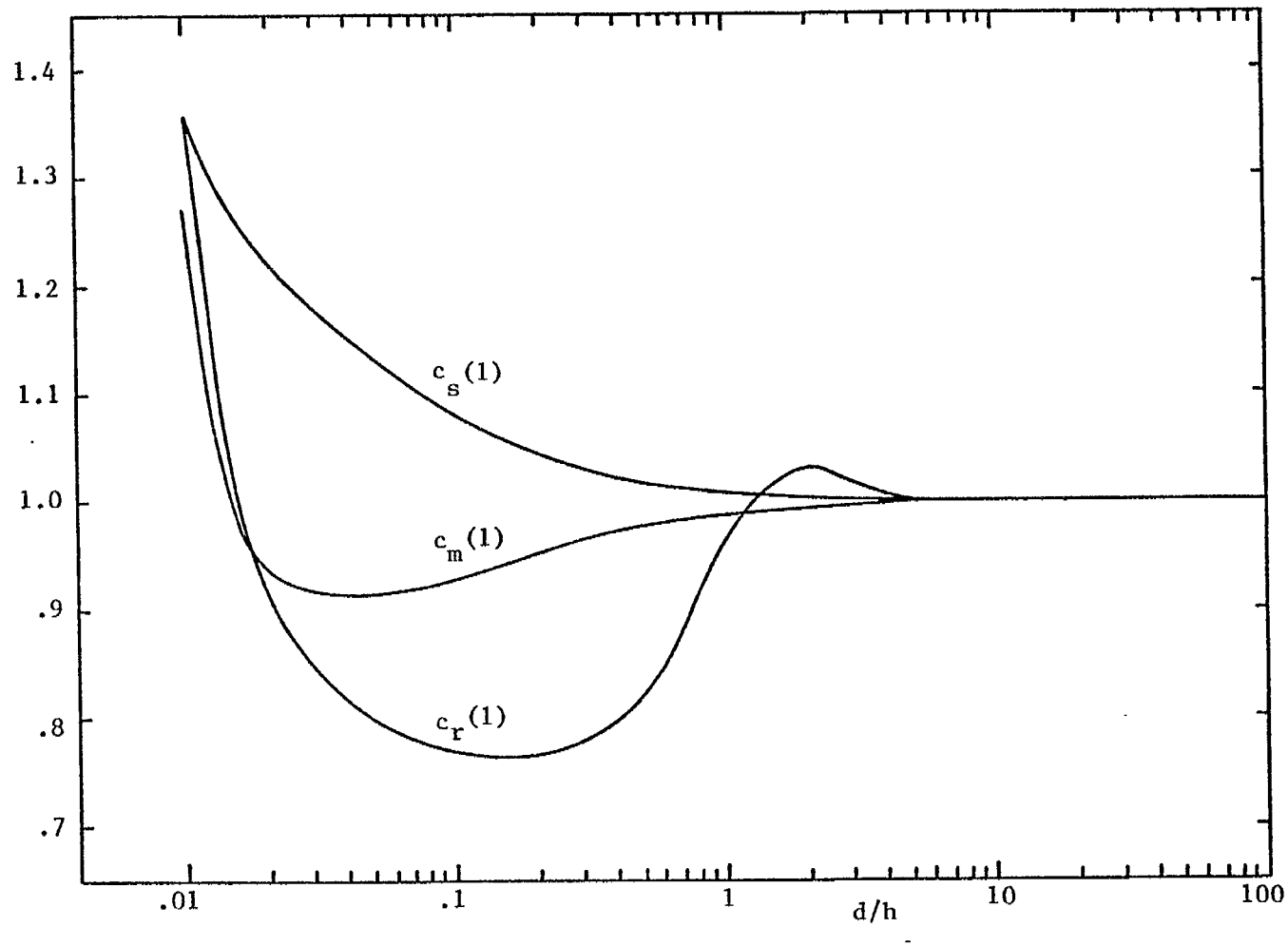


Figure 19. The field enhancement factors at the upper end of the post.

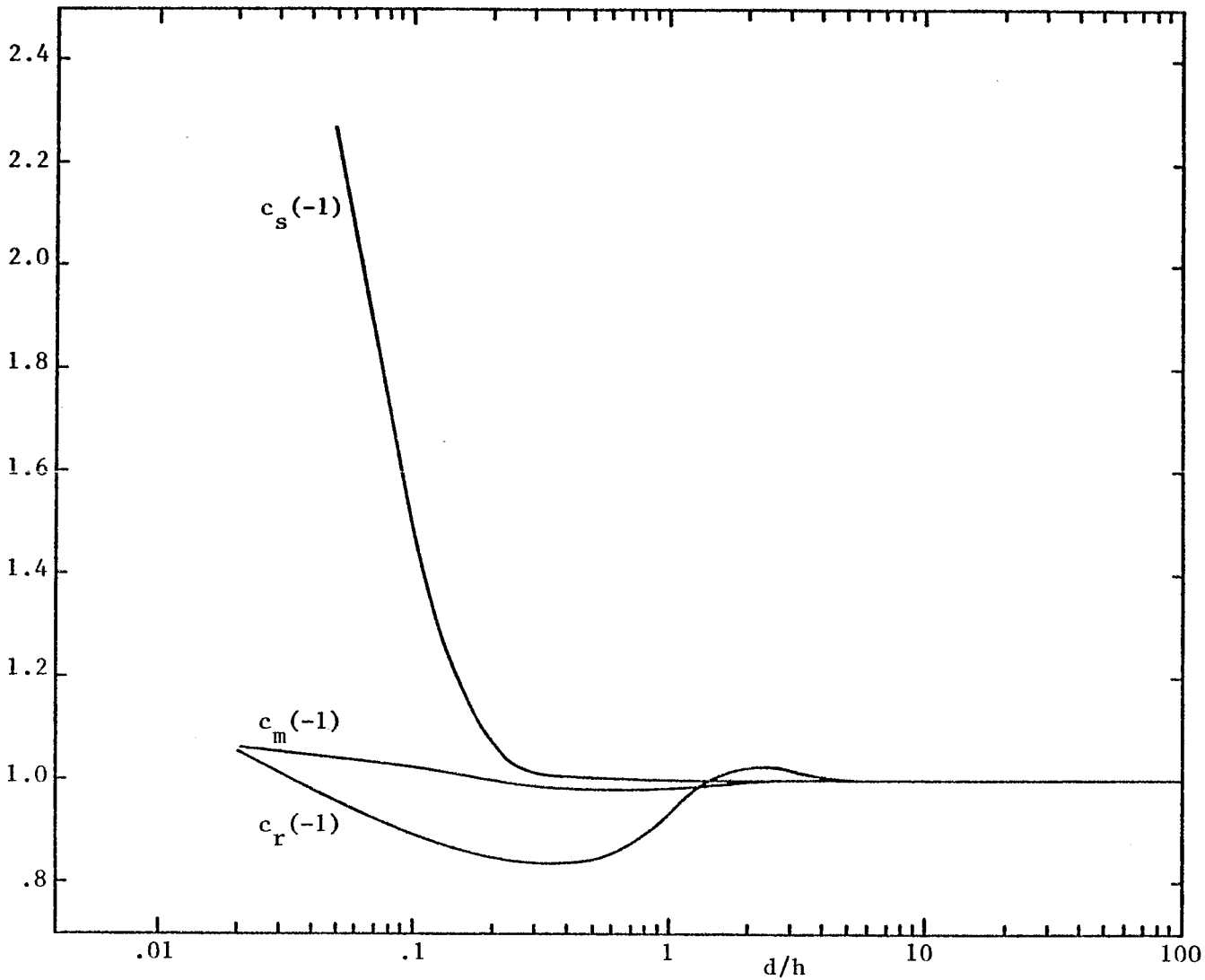


Figure 20. The field inhancement factors at the lower end of the post.

Acknowledgment

We wish to thank Mr. R. W. Sassman for his indispensable assistance in the numerical computations, Capt. C. E. Baum and Dr. K. S. H. Lee for their suggestions, Mrs. G. Peralta for typing the manuscript, and Mrs. E. Ravndal for preparing all the figures.

## References


1. R. W. Latham, K. S. H. Lee and R. W. Sassman, "Minimization of Current Distortion on a Cylindrical Post Piercing a Parallel-Plate Waveguide," Sensor and Simulation Note 93, September 1969.
2. R. W. Latham and K. S. H. Lee, "Electromagnetic Interaction Between a Cylindrical Post and a Two-Parallel-Plate Simulator, I," Sensor and Simulation Note 111, July 1970.
3. K. S. H. Lee, "Electromagnetic Interaction Between a Cylindrical Post and a Two-Parallel-Plate Simulator, II (a Circular Hole in the Top Plate)," Sensor and Simulation Note 121, November 1970.
4. L. Marin, "A Cylindrical Post Above a Perfectly Conducting Plate, I (Static Case)," Sensor and Simulation Note 134, July 1971.
5. R. W. Sassman, "The Current Induced on a Finite, Perfectly Conducting, Solid Cylinder in Free Space by an Electromagnetic Pulse," EMP Interaction Note 11, July 1967.
6. C. D. Taylor and G. A. Steigerwald, "On the Pulse Excitation of a Cylinder in a Parallel Plate Waveguide," Sensor and Simulation Note 99, March 1970.
7. C. E. Fröberg, Introduction to Numerical Analysis, Addison-Wesley, New York, Second Edition, 1969.
8. M. Abromowitz and I. N. Stegum, Editors, Handbook of Mathematical Functions, National Bureau of Standards, AMS-55, 1964.